2018•2019

Faculteit Industriële ingenieurswetenschappen

master in de industriële wetenschappen: elektromechanica

Masterthesis

Characterizing bulk and interface behavior of encapsulants within photovoltaic laminates

PROMOTOR :

Prof. dr. ir. Michael DAENEN

PROMOTOR :

Dhr. Philippe NIVELLE

Busra Sesli

Scriptie ingediend tot het behalen van de graad van master in de industriële wetenschappen: elektromechanica

Gezamenlijke opleiding UHasselt en KU Leuven

2018 • 2019

Faculteit Industriële ingenieurswetenschappen

master in de industriële wetenschappen: elektromechanica

Masterthesis

Characterizing bulk and interface behavior of encapsulants within photovoltaic laminates

PROMOTOR :

Prof. dr. ir. Michael DAENEN

PROMOTOR :

Dhr. Philippe NIVELLE

Busra Sesli

Scriptie ingediend tot het behalen van de graad van master in de industriële wetenschappen: elektromechanica

UHASSELT

KU LEUVEN

Acknowledgements

After four years of hard work and determination, this wonderful journey has come to an end with this master's thesis. I certainly was not alone in this adventure, therefore i would like to give special thanks to a number of people for their support and advice.

First of all I would like to thank prof. dr. ir. Michaël Daenen his supervision during my bachelor and master studies, his patience and giving me useful advices. It was a pleasure to work with a person with such greatness and intelligence. Thanks to my valuable promoter Philippe for his guidance, interest and suggestions. Thanks to Jorne for his motivation and support. I would also like to show my appreciation towards all my professors that guided me with their experiences during my bachelor and masters studies.

Also, thanks to my colleagues from EnergyVille for all their help. Further, I would like to thank my family who contributed in so many different ways, not only during my thesis work but also through my entire studies. They always encouraged me and provided emotional support. Last but certainly not least, I am very grateful to my friend Cem, Yeliz for their help and support and for cheering me up during difficult times.
I appreciate everyone that helped me to achieve my goals.

Busra Merve Sesli
August 2019

Table of Contents

List of Figures

Abstract

With the technology of today, more widespread implementation of Photovoltaic is possible by integrating it in buildings, vehicles and other infrastructures. Since these applications require a long lifetime, the reliability amelioration is essential.
Climate-induced degradation modes will affect the efficiency, stability and lifetime of the photovoltaic (PV) modules. Among the most common degradation modes, the most prevalent one is the failure of the interconnection, followed by delamination. Delamination can occur between different components in the PV-laminate. However, in the case of encapsulant-cell delamination, it seems to happen selectively around the interconnections and screen-printed contacts. The objective of this master thesis is to study delamination by characterizing the parameters which contribute to the adhesion between the interconnection and the encapsulant.

According to the literature, the roughness of a surface is a key parameter that has a significant influence on the adhesion strength. It has also been shown that the effect of roughness is influenced by the mechanical behavior of the adhesive. Therefore these two parameters are studied to characterize the adhesion. Primarily, the adherend surface is characterized completely with a confocal laser scanning microscope. Subsequently, the mechanical properties of the encapsulant are determined by using the technic of dynamic mechanical analysis. A material model is fit to the experimental results to use this as an input for reliability models. Furthermore, the influence of process parameters, various encapsulants as well as the different metal contacts are examined with a scanning electron microscope. Finally, by accelerating the degradation modes and determining changes at the interface more insights are gained on the thermomechanical stress induced at the interfaces within PV laminates.

Samenvatting

Met de technologie van vandaag is de implementatie van Fotovoltaïsche zonnepanelen (PV) in bredere toepassingen zoals integratie in gebouwen, voertuigen en andere infrastructuren mogelijk. Sinds deze toepassingen een lange levensduur nodig hebben, is het essentieel dat de betrouwbaarheid steeds verbeterd wordt. Degradatie door weersomstandigheden is een problemen die de betrouwbaarheid en de efficiëntie van een PV-module kunnen beïnvloeden.

Degradatie van de metalen onderdelen is de meest voorkomende vorm van degradatie. Een ander belangrijke type van degradatie is delaminatie. Deze kan tussen verschillende componenten in de PV-laminaat ontstaan. Echter, in het geval encapsulant-cell delaminatie gebeurt het selectief rond de metallische contacten. Het doel van deze master thesis is het bestuderen van de delaminatie door de parameters te karakteriseren die bijdragen tot de adhesie tussen metalen contacten en de encapsulant.

Uit de literatuur blijk dat de ruwheid van een oppervlak een belangrijke parameter die een significante invloed heeft op de adhesie tussen twee oppervlakken. Het is ook aangetoond dat de mate waarin ruwheid een invloed heeft, afhankelijk is van de mechanische eigenschappen van de encapsulant. Hiervoor zijn deze twee parameters onderzocht om de adhesie te kunnen karakteriseren. Eerst is een volledige karakterisatie van het oppervlak gedaan met een confocale lasermicroscoop. Hierna zijn de mechanische eigenschappen van de encapsulant bepaald met behulp van een rheometer. Een visco-elastisch materiaalmodel werd gefit op het experimenteel bekomen resultaat, om deze vervolgens als input te gebruiken voor betrouwbaarheidssimulaties. Ook is de invloed van de procesparameters, de verschillende soorten encapsulanten en de verschillende soorten metalen contacten onderzocht met behulp van een electronenmicroscoop. Tenslotte wordt het effect van de thermomechanisch geïnduceerde stress onderzocht door de degradatie mechanismen te versnellen en de veranderingen op de interface vast te stellen.

Chapter 1

Introduction

Energyville is a collaboration between the Flemish research partners KU Leuven, VITO, imec and UHasselt in the field of sustainable energy and intelligent energy systems[1]. The research group Energy Systems Engineering (ESE) from UHasselt investigates the reliability of renewable energy supply. Currently, the main focus of this group is the reliability of photovoltaic systems[2]. In this Masterâs thesis the influence of the encapsulant on the reliability of photovoltaic modules is studied.

The electricity production from solar and wind energy is uncertain and not always reliable compared with conventional energy sources, due to its dependence on the weather. However, there are various forms of renewable energy that are reliable enough in order to increase the share of renewable energy.[3]

During the development of PV systems, a higher efficiency is targeted. Since the theoretically possible limits of the current commercial systems have almost been reached, the target becomes ever more difficult. There are several ways for an energy technology to become more competitive and hence also more cost efficient. Levelized cost of enegy (LCOE) is a way to compare the potential of different technologies.

The LCOE is an economical term that tells what the total cost is to win energy out of a certain energy system during its lifespan. This is calculated by summing all the costs of the system during its lifecycle and dividing this sum by the total produced electrical energy. The values of the LCOE is used the compare different renewable energy technologies.[4]

The performance and lifespan of a PV-module is determined by its subparts, the subparts of a standard silicon PV-module are shown in Figure 1 1. The top and bottom layer provides mechanical protection and is made out of glass and backsheet, respectively. For bifacial solar panels these both layers have to be transparent. This means that also the bottom layer has to be in glass. Below the glass and on top of the backsheet one can find the encapsulant. This is a polymer with various functionalities:

- Binding element for the subcomponents
- Protect the cell against moisture
- Optical coupling.

The polymer has to provide optical coupling to the Si-cell, which means that it has to be transparent for a broad spectrum of the light. Between the encapsulants the Si-cell is located together with the interconnection. The interconnection converts the incoming light into an electric current. On the silicon one can find the so-called fingers, which are metal strips in which the current is

accumulated and transported to busbars. These busbars then direct the current outside.[3]

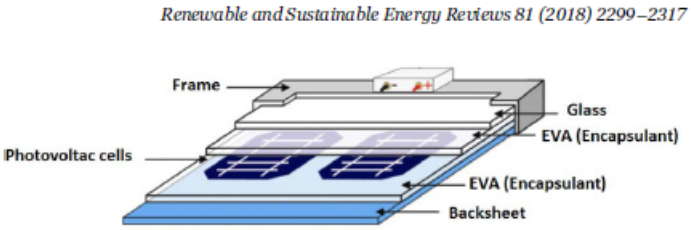

Figure 1.1: Components of a standard Si-PV-module.[3]

1.1 Problem Statement

From a PV-system it is expected to hold its energy yield for at least 25 to 30 years. This implies that a PV-system has to be able to provide 80% of its initial power during its first 30 years. In order to increase the use of PV-systems, people are working on integrating PV in the facade of buildings (BPIV). In this way, existing infrastructures can be used to generate energy. However, this would require a minimal lifespan of 50 years for the PV-system.[1,3]

Therefore, it is important to continuously increase the reliability of PV-systems. Nevertheless, the PV-module can be considered as the most reliable part within the whole PV-system. There are different failure possibilities for a PV-module. For example, it is known that approximately 40% of the failures is due to the interconnection [5]. The main cause behind the different failure mechanisms are related to moisture. Moisture in combination with UV light corrodes the metal parts such as the interconnection. It also causes delamination and the loosening of the encapsulant.[6]

As shown in Figure 2 1, the interconnection is the most sensitive part of the module. However, its failure is often traceable back to the interaction with the encapsulant. In order to increase the reliability of the interconnection it is thus important to understand and get insight in the role of the encapsulant. Since the encapsulant glues the different components together, it is the encapsulant that mainly determines the thermomechanical behaviour of the PV-module. This behaviour is determined by:

- The connection between the different components
- The differences in the thermal expansion coefficients within the region where the encapsulant dominates.

The loss in attachment between the encapsulant and the interconnection changes the stress distribution inside the module, which can be disadvantageous in the long term.

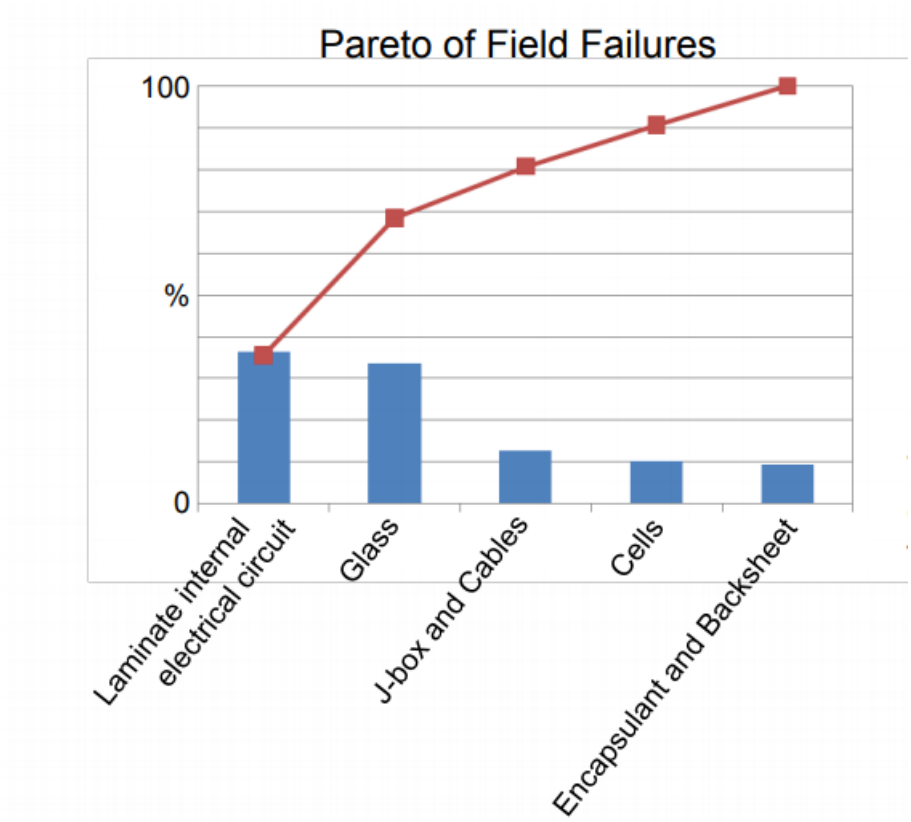

Figure 1.2: Percentage failing parts[7]

1.2 Objectives

The main objective of this Master's thesis is to investigate the role of the encapsulant in the reliability of a PV module. As mentioned in the problem statement, it is essential to study the adhesion between the various components. For this, the way in which the encapsulant interacts with the interconnection metallization must be studied. The first sub-objective is therefore to study and experimentally examine the different parameters that have an influence on the adhesion behavior. Since different types of encapsulants are used, three different types are tested.

A further sub-objective is to determine the influence of the adhesion behavior on the module level. Once insight has been gained into the various parameters that have an influence on the adhesion behavior of the encapsulant, these can be used as an input for finite element simulations. With these simulations the effects of the various parameters at module level become visible. In this way, the simulation can be used to show where the PV module will begin to fail under the influence of a certain load.

1.3 Methodology

First, a literature study is performed to determine the parameters that influence the adhesion behavior of the encapsulant.

For example, various studies can be found that show that the roughness of the surface has a major influence on the adhesion behavior of the polymer on that surface. An important parameter is therefore the determination of the root mean square (rms) roughness value of that surface [5]. This parameter will, among other things, be determined for all components of the interconnection using a 3D confocal microscope.

In addition, there are other factors as surface energy, rheological parameters, capillary forces and electrostatic contributions that must be taken into account when studying the adhesion properties of a surface [5]. These can be characterized using chemical analysis techniques such as the Fourier Transform Infrared Spectroscopy (FTIR) or X-ray diffraction (XRD).

Other important parameters are the pressure and temperature of the lamination process. The pressure at which the lamination takes place has one-on-one influence on how far the polymer will penetrate into the metallization: the higher the pressure, the deeper the polymer can penetrate into the surface of the metallization. The temperature determines the viscosity of the polymer and thus also has an influence on the penetration of the polymer into the metallization. Another parameter is the process time. It must be kept constant to give the polymer time to cure. The curing process of the polymer has an influence on the physical and chemical properties of the polymer.[9]

To determine the influence of the parameters of the lamination process, mini PV-modules can be made in which one parameter is changed each time. At least three different polymers will also be used as encapsulants. The reason for using mini PV-modules is primarily a matter of saving material, since PV-modules are relatively expensive. However, the behavior of the mini modules remains representative of standard PV-modules. The mini PV-modules can then be cut to study the interaction of the polymer with the metallization under the optical microscope. A chemical analysis will also be done using XRD.

Dynamic mechanical analysis will be carried out to determine the time-temperature dependence of viscoelastic behavior of the adhesives. The influence of the mechanical properties on the adhesion system will be investigated.

The parameters found will then serve as input for the finite element simulations. On the basis of these simulations, the effects of the stress load on the module level can be made visible. These simulations must then be validated by loading the PV-modules using the accelerated stress tests. Sensors will be incorporated into the laminate to quantify temperatures and stress.

Chapter 2

Literature Review

2.1 Photovoltaic module

2.1.1 Photovoltaic effect

A solar cell is a wafer of silicon of which the top layer is phosphorous doped silicon (N-type), and the bottom layer is boron-doped (P-type). While the n-type layer has an excess of electrons, the p-type layer has positively charged holes. Therefore, at the region where the two layers meet, an internal electric field, the depletion region, is created. Now, if sunlight hits the silicon wafer and penetrates to the depletion region, electrons are excited to a higher level of energy which due to the created electric field is prevented to recombine again with a hole. The electrons and holes can combine via another pathway, which is going to be the electrical circuit. Then, the energy dissipates in the electric circuit and like this, the photons of solar energy are converted to DC-current and voltage. This is the so called photovoltaic effect.[10]

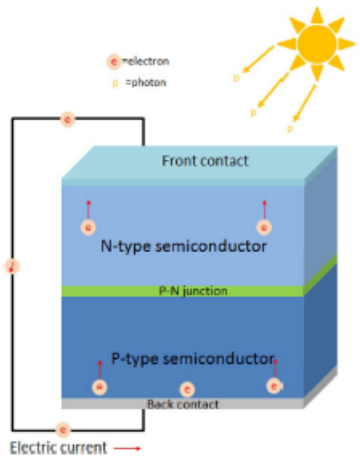

Figure 2.1: principle of photovoltaic effect.[10]

2.1.2 Characteristics of the Si-PV module

The structure of a typical PV-laminate exists out of the different components. The most top and bottom layers are glass and along the backside, this serves as protection against impact and electrical insulation. Along the backside, there is a backsheet or glass as coverage. Under the glass and above the backsheet (or glass), there are layers of encapsulant. Finally, between the two encapsulant layers, there is a silicon cell with metallization. In the silicon-cell, the conversion of light to current takes place. Subsequently, the generated current is collected in small metal lines,

which have a dimension of 2 mm, also referred to as fingers. This metallization is applied on the Si-cell mostly by the technique of screen printing. Other used techniques are inkjet printing, pad printing, stencil-printing, pad-printing, dispensing technology, photolithographic and evaporation process, laser micro-sintering, and plating. Subsequently, the current is lead to the busbars which provide the connection between different cells.[3]

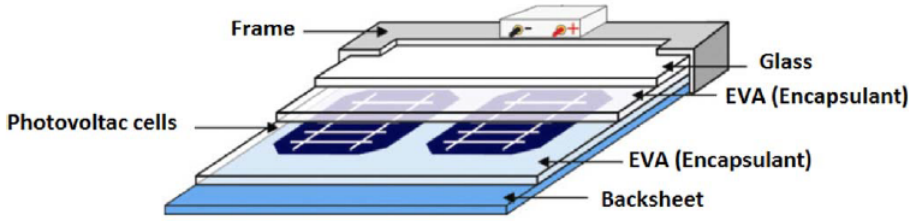

Figure 2.2: Components of a standard Si-PV-module.[3]

The protection of the Si-cell is an important aspect of the PV-module. This Si-cell is a thin wafer with a thickness of around 180 micrometers and an area of 156x156 mm2, which is relatively big in proportion, and therefore very fragile. Therefore, it is hermetically sealed with encapsulant, which has different functions to fulfill besides the absorption and damping of the mechanical stresses. The encapsulant also serves as structural support and positioning of the solar cell in the module layout.

Next, the encapsulant also have to be electrical resistive properties, the insulation of the cells can prevent electrical short circuits due to leakage of current . Since the PV-modules are located outside, they should be resistant against outside conditions, thus the encapsulant has to be resistance to UV-radiation, water ingression, temperature variations and it has to be a physical isolation for the cells from the outside conditions. However, it is reported that mostly due to these factors; Moisture (moisture, dew, fog, rain), heat and UV, the encapsulant undergoes physical and chemical degradation.

Further, the encapsulant is the layer above the Si-cell, thus it serves also as an optical coupling. The transmission of a broad spectrum of light is an important property since all the light that is absorbed by the encapsulant is light that can not be converted in current and thus will be a loss. Moreover, properties as volume resistivity, relatively low crosslinking temperature and high adhesion strength are also of relevance.[3]

2.1.3 Degradation mechanism of the Si-PV module

It is reported that, among the most common field failures, the most prevalent one is delamination, followed by corrosion [11]. The degradation of the polymer causes delamination due to climatic factors as moisture, temperature, UV radiation or other environmental conditions as mechanical stresses and electrical operating conditions, pollutants/gases, sand, dust, wind, are some examples. There are different degradation mechanisms, while one or more of these factors can be the underlying cause. The different factors have a cooperative effect on the failure modes of a PV-module. The by-product of one degradation mode can trigger other degradation mechanisms. The different degradation modes result in a drop in module efficiency. [3]

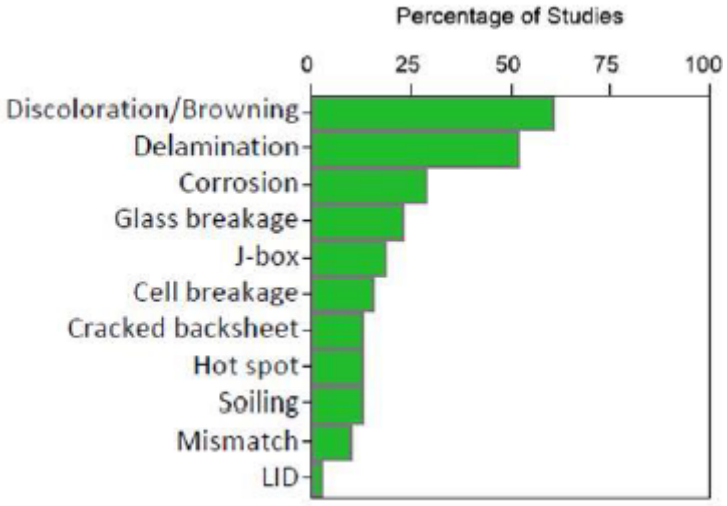

Figure 2.3: Observed changes of PV-modules in the field. [8]

One of the significant degradation mechanisms to which encapsulants are susceptible is photodegradation — the process of changing the structure of the polymer due to UV-radiation. The energy of the UV-radiation that permeates the encapsulant has enough energy to break the chemical bonds and create free radicals. This effect is enhanced when the temperatures elevate. When photodegradation takes place in an oxygen-rich atmosphere, the free radicals will setup an auto-oxidation process. With consequent of the degradation of the polymer which leads to delamination and yellowing of the encapsulant. These effects, in turn, cause moisture ingress and loss of optical transparency.

In the case of the most used encapsulant, EVA, the photodegradation causes the formation of acetic acid (HAc). The produced acetic acid is self-catalyst, while adding free-radical inhibitors to the encapsulant does not seem to retard the formation, which makes the effect more severe. Besides causing delamination, the produced acid attacks the metal contacts by corrosion. In addition to this, delamination of the encapsulant enhances moisture ingress, which leads to corrosion of the contacts. Also, exposing the EVA to water decomposes the polymer, producing similarly, acetic acid. Moreover, the acid causes a decrease in the pH that also enhances the effect of corrosion.

Photodegradation impacts optical properties due to changes in the polymer structure, which can lead to crystallization of the microstructure and as a result of this to loss of transparency. Another way it affects transparency is by an increase in reflection.
Another degradation mechanism that affects the reliability of the PV-module in different ways is moisture ingress. Water vapor molecules are very reactive, and the interaction with polymer molecules causes hydrolysis - the chemical breakdown of the material. When it interacts with the metallization on the cell, it induces corrosion of the metallization. Chemical reactions also release gases which cannot escape the encapsulant. These gases give rise to bubble formation or locally delamination of the encapsulant. The formation of bubbles affect the module in different ways; the entrapped air hinders the dissipation of heat; the reflection of light increases. Thus moisture is a promotor for corrosion, delamination and yellowing of the encapsulant.

Although encapsulant materials should be resistant to moisture, it is not possible to completely prevent moisture ingress. However, the accumulation of liquid water is inhibited by good adhesion. Therefore, good adhesion qualities are considered to be more important than resistivity to moisture.

High temperatures, as well as changes in temperatures in short periods, impacts the reliability of

the modules. Especially the mechanical properties of polymeric materials, as well as the electrical and optical properties, are prone to changes in temperatures. Besides, the change in temperatures induces thermomechanical stress in the modules. The induced stress in the module gives rise to differences in adhesion and can lead to delamination.[3,6,8-9]

Fig. Illustrates the delamination on a photovoltaic module that appears around the metallization and busbars of the cell. The corrosion of the metallization happens at the places where the encapsulant is delaminated.

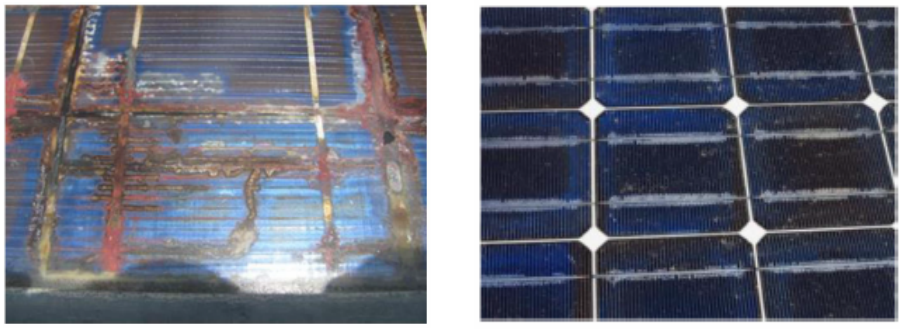

Figure 2.4: Delamination between cell and encapsulant especially around the metallization (left) [9] Corrosion of the metallization due to delamination(right)[11]

2.2 Adhesion

Adhesion is the state where two substrates are stuck together by only surface attachment which involves physical and chemical mechanisms. When the two substrates are stuck together, a contact region or an interface is formed. The adhesive is the substrate that is capable of holding the materials together and the adherend is the substrate on which it holds. In addition, the adhesive should also transfer and distribute the load through the other components on which it is attached.

2.2.1 Mechanisms of adhesion

Different theories describe the mechanisms of adhesion. These are mechanical interlocking, adsorption, electrostatic attraction and diffusion. Adhesion between two substrates is mostly ascribed to a combination of mechanisms, and even the individual contributions may be difficult to determine. The most frequently considered mechanisms are mechanical interlocking and adsorption. However, there are applications whereby the last two theories, namely the diffusion theory and electrostatic theory, can only explain the adhesion.

The mechanical theory of adhesion describes the interlocking effect between adhesive and adherend. Applying a low-viscosity adhesive to a surface fills all the irregularities and cavities. Subsequently, when the adhesive hardens, a form-locked connection is created.

Generally, mechanical interlocking at macroscopic-level and microscopic-level are distinguished. However, it should be noted that mechanical interlocking at the macroscopic-level generally has little contribution to the adhesive bond. On the other hand, mechanical interlocking at the microscopic level is of great importance for the adhesion as it is discussed under the heading roughness effect.

One of the most common examples of mechanical interlocking at the macroscopic level is dental filling. The amalgam filling has good cohesive properties but poor adhesion to the tooth. Making an undercut in the tooth to create an anchor effect provides the bonding. Also, for micromechanical adhesion, tooth filling can be given as an example. Before applying the filling, the tooth is chemically etched to create micro-holes that can be filled afterward with the filling.

The adsorption theory states that there are forces between the adhesive and adherend to form intermolecular bonds, which result in adhesion. There can be made a distinction between chemical adsorption or chemisorption when there is a primary bond between the surfaces, and physical adsorption, those are secondary bond formation due to van der Waals forces. Adhesion due to the secondary forces is sometimes treated under the heading of electrostatic attraction.

This mechanism is especially of importance because it is always present even when there are no reactive groups present in the interface to form a physical bonding. The London dispersion forces result from the motion of electrons that creates temporary dipoles. These forces are the weakest forces but always present. The more general term for these weak interactions is the Van der Waals forces; it includes the interaction between a permanent dipole-induced dipole and permanent-permanent interactions. Although these forces are negligible in comparison, they are sufficient to have a reasonable strength of adhesion. However, these forces are very short-ranged; the force decreases with the 6th or 7th power of the distance. Thus, there needs to be intimate contact between the substrates, which is not always possible. The adsorption theory tells us that whenever there is intimate contact between two surfaces, there are forces of attraction between them. However, there is a need to have sufficiently intimate contact between the two substrates since these forces lose significance beyond 0,5 nm.

The electrostatic theory states that an electrical double layer exists at the interface between the

two substrates. Mostly, this theory is applicable in the case of two metal substrates; electrons are transferred from one to another to form the double layer. As mentioned above, sometimes the intermolecular bonding due to the secondary forces is also involved in the adsorption theory.

Lastly, The diffusion theory is mainly useful in the case of polymer-polymer adhesion and is of minor significance in the case of polymer-metal adhesion. The mechanism on which this theory relies is the diffusion of one substrate in the other. In the case of polymers, the entangling of the polymer chains of the adherend and adhesive provides the bonding.[12]

2.2.2 Strength of adhesion

A very intuitively approach to describe the quality of the adhesion is to tear the surfaces from each other and define the load that the joint can bear before breaking. This approach is referred to as practical adhesion. However, it is not the intrinsic property of an adhesive that is measured in this way but the response of the adhesively bonded assembly to destructive deformation. Besides the interfacial forces, the mechanical properties of the adhesive, adherend and the surface regions or interface influence the strength of the adhesion. Hence, the energy needed to separate two surfaces is much higher than the energy needed only to overcome the interfacial forces. Thus a difference between practical adhesion and theoretical adhesion should be made.

Bonded joints are complex assemblies because the properties of the adhesive, as well as the adherend, influence the strength of adhesion. Thereby the joint geometry and the deformation characteristics affect the stress distribution through the joint and thus the strength. Fig. illustrates the most common adhesive testing methods; tensile test, peel test and the shear test. As an example, there is energy dissipated in stretching of the adherends when a shear test is performed and thus the E modulus of the adherend affects the result, while during the peel test there is also dissipation of energy in bending of the adherend. Therefore, the numerical results obtained for adhesion strength vary dependent on the test. Even for the same type of joint different numerical results can be obtained, as factors of operational parameters affect the results. Since polymeric adhesives show a viscoelastic behavior, the rate of loading is one of these factors. Also, the dimensions of the sample play a role while this effect varies depending on the joint.

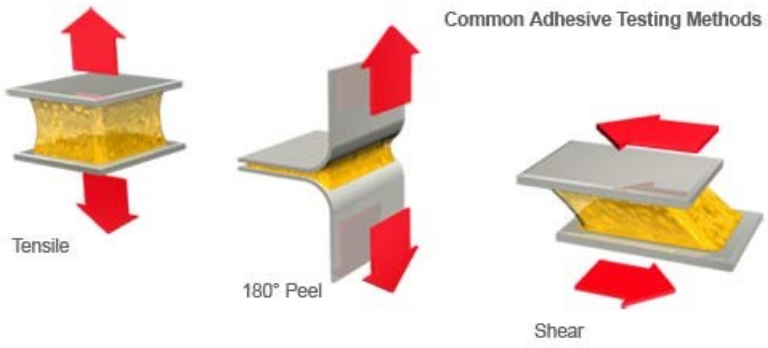

Figure 2.5: most common types of adhesive testing.[13]

Furthermore, there are different ways to load the joint. One can load the joint in tension, shear, compression, or a combination of these. As adhesive joints are composite structures, even simple loading modes as tension, compression or shear give rise to much more complex non-uniform stresses in the joints that are absent in the external loading, this is illustrated in fig.. Therefore, the data is not reliable because ideally, there is a need for a unique relationship between the load applied and the magnitude of the measured stress. The complex stresses that arise in the joint can cause locally induced stress concentrations rather than a uniform stress state through a region of the joint. Hence, these stress concentrations lower the strength of adhesion. The locus of failure

affects the magnitude of the force that the joint can bear before failing, as the amount of energy dissipated depends on the way the bond fails.

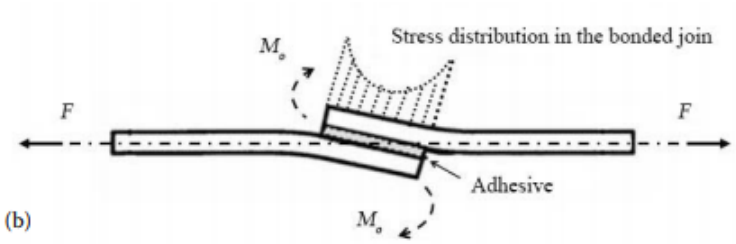

Figure 2.6: Stress distribution of a single lap joint.[14]

Finally, the different ways to fail for an adhesive bond are a cohesive, adhesive, or interfacial failure. A cohesive failure occurs when the material fails in the bulk. The adherend, as well as the substrate, can fail cohesively. If the bond fails at the interface, it is called an adhesive failure. It can also happen that the failure is a combination of the two. In either case, it is essential to analyze the fracture area to determine the locus of failure. All these factors make it very complex to interpret the values obtained from the results of a strength test. Therefore, the results obtained from these tests are mainly comparative.[13-18]

The fundamental adhesion or theoretical adhesion is the energy needed to form the bonds between the substrates. Ideally, if no other energy dissipating processes are accounted, this energy is equal to breaking the bonds and form two separate surfaces. This ideal scenario could be the case for perfectly brittle materials. The fundamental adhesion can thus be described with thermodynamically reversible equations, also referred to as work of adhesion:

$$W_A = \gamma_1 + \gamma_2 - \gamma_{12} \tag{2.1}$$

With W_A the work of adhesion, γ_1 the free surface energy of surface 1, γ_2 that of surface 2 and γ_{12} the interfacial energy between the two phases.
The energy needed to break cohesively within the material is (W_C) :

$$W_C = 2\gamma_1 \tag{2.2}$$

These are reversible thermodynamic equations the energy that will be needed to form two separate surfaces. Since this is an ideal scenario and no energy dissipating processes are involved, the bonding energy equals the debonding energy.

Although a difference is made between practical adhesion and theoretical adhesion, these are not unrelated. The following equation can be seen as a simple link between practical adhesion and fundamental adhesion.

$$G = G_0 + \psi \tag{2.3}$$

With G_0 representing the fundamental adhesion, ψ the other energy absorbing processes and G the total energy. However, the relationship is not as simple as it is seen, there is also an relationship between the fundamental adhesion and the energy absorbing processes. Otherwise the G_0 term could just have been neglected since it is a few orders less in magnitude than ψ. However, the relationship between those two is not directly measurable and depends on the assembly.[19]

2.3 Factors that influence adhesion

2.3.1 Wetting

Intimate contact is necessary for good adhesion, regardless of the mechanism of adhesion. The process of creating continuous contact between surfaces is also called wetting. The wetting behavior of a liquid on a solid substrate depends on its affinity to the solid material. Every material has an associated surface energy, which is dependent on its chemistry, that impacts its adhesion to itself and other materials. When the surface free energy of the adherend is higher than the surface energy of the adhesive, spontaneous spreading occurs to wet the surface completely.

The free surface energy of a solid can be considered as the energy needed to create a new surface in the material. The reason why the atoms at the surface have a higher energy state is that they have some dangling bonds that could not interact with other atoms. On the other hand, the atoms in the bulk material are surrounded by other atoms and interact with them, lowering their energy state. Moreover, if the energy at the surface would be less than the energy in bulk, there would be a continuously driving force to create surfaces.

A concept closely allied with surface energy is the surface tension. It is defined as the force per unit length that acts perpendicular to any line in a liquid surface. Thus, the force needed to increase the surface area of the liquid. The surface tension and surface energy are equal if the free surface energy does not change while increasing the surface area of the liquid. In some cases, as in multi-component liquids, these two terms cannot be considered equal. However, these two terms, as well as the symbol y, are mostly used as if it is interchangeable.

Although these terms are introduced related to the material itself, a surface cannot exist on its own. Thus the term surface energy without qualification is, technically, the energy measured in vacuum. The surface tension between any two surfaces is the interfacial tension. In the case of a drop of liquid on a solid substrate surrounded by a fluid, in the most cases air, the surface tensions are illustrated as vectors in fig. The contact angle determines the wetting behavior of the liquid. Whereas an angle of 90 degrees correlates to wetting, angles more than 90degrees accord to non-wetting behavior. When the angle is 0 degrees, spreading occurs. The young equation describes the balance of the different surface tensions :

$$\gamma_s v = \gamma_s l + \gamma_h v \cos\theta_\gamma \tag{2.4}$$

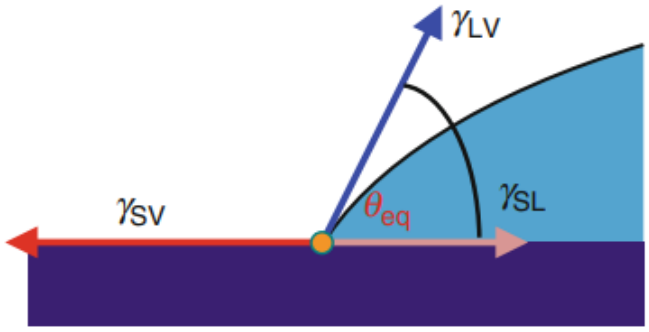

Figure 2.7: Three phase equilibrium of surface tensions. [21]

Besides the surface chemistry, there are the physical characteristics of the surface that determines the wetting behavior. Every surface has roughness on different length scales, and this will

alter the contact angle compared with the idealized case of a smooth surface. Thus a correction factor is needed for the preceding equations. This correction factor r is the ratio of the real area to the projected area. The corrected contact angle takes into account the roughness but it also makes the assumption that complete wetting occurs and there are no inhomogeneities. This type of wetting is called the Wenzel state and is stated by the following equation:

$$\cos\Theta_m = r\cos\theta_\gamma \tag{2.5}$$

The roughness always amplifies the effect of wetting or dewetting because the correction factor is always equal to or greater than one, since all surfaces have roughness to some degree.

However, if no complete wetting occurs due to gas entrapment in the holes or other inhomogenities, the Wenzel state is not valid. In that case the wetting is described by the Cassie-Baxter state and stated with the following equation in the most general form:

$$\cos\Theta_m = x_1\cos\Theta_y 1 + x_2\cos\theta_y 2 \tag{2.6}$$

With x the fraction of area and theta the angle, whereby the subscription 1 and 2 refer to the different surface chemistries. In the most case is one of the surface chemistry, air. Since in this case the droplet sits on the top of the asperities and the surface area is much less compared to the Wenzel state, this type of wetting relates to hydrophobicity.
Fig. illustrates the Wenzel state and the Cassie-baxter state.

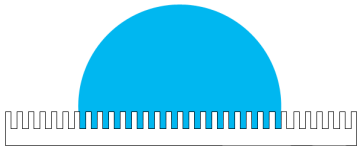

Figure 2.8: Schematically illustration of the Wenzel state.[21]

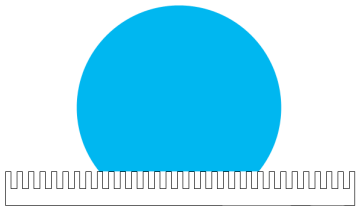

Figure 2.9: Schematic illustration of the Cassie-Baxter state.[21]

It is also demonstrated their depth, aperture angle and diameter of the pores also play a role in the penetration of the adhesive in the holes. A result of the classic work of the Bruyne shows that the ink bottle shaped pore is particularly difficult to wet, fig .

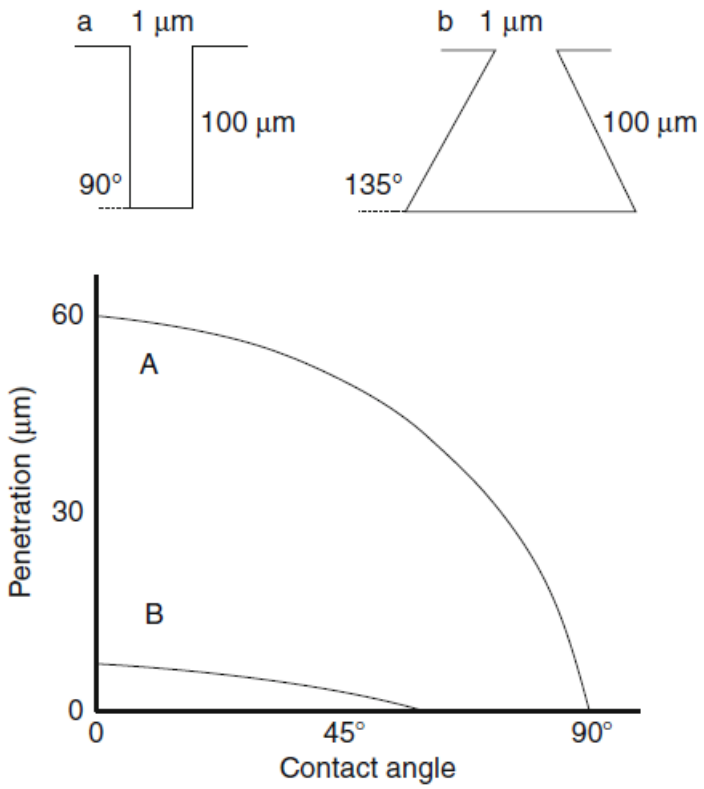

Figure 2.10: Stress distribution of a single lap joint.[22]

The viscosity of the adhesive and the counterpressure of the trapped gas in the holes also affect the penetration of the adhesive to the adherend.[12,18-22]

2.3.2 Roughness

Even the weakest forces, which are always present in all matter, namely the van der Waals forces, are enough to provide a really strong bond, nevertheless, adhesion is not usually observed. This is often referred to as the adhesion paradox. The adhesion gets vanished by the presence of adhesion. However, the relationship of roughness and adhesion is rather a complex one. Although roughness can have a negative impact on adhesion between substrates, it can also improve it. If the adhesion is enhanced or negatively influenced, mainly depends on the wetting. In fact, it can be said that roughness affects the adhesion in two ways. First, the adhesion mainly depends on the effective area, which implies more fundamental adhesion. Second, the roughness relates to adhesion through mechanical interlocking mechanism.[23-24]

One of the most popular example that illustrates the vanishing of adhesion due to surface roughness is the so called lotus effect. This effect describes the minimizing of the adhesion to a surface by tuning the architecture of the surface. When a surface is randomly rough and causes high contact angle hysteresis, the liquid is not able to wet the surface. This allows air to be entrapped which adversely affect the wetting. This makes the liquid dangling on the top of the asperities with as consequence much less contact area and a very large contact angle. Fig. illustrates how the combination of roughness at micro scale and the nano scale cause a non-wettable surface.[21,25]

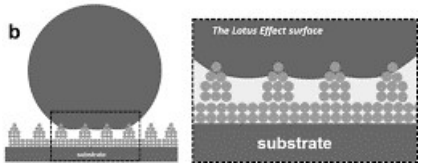

Figure 2.11: Illustrative example of the Lotus effect[26]

The so called petal effect, on the other hand, shows that despite the large contact angle that the liquid makes with the surface, there is perfect wetting at nanoscale and thus adhesion, fig..

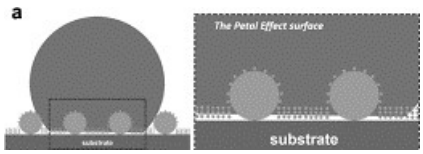

Figure 2.12: Illustrative example of the Pettal effect[26]

The enhancement of the adhesion with roughness relates to the mechanical interlocking mechanism of adhesion on the one hand. The roughness at the microscopic level provides irregularities or porosities to enhance the interlocking effect. On the other hand, the fundamental adhesion is also ascribed to an increase of effective area and therefore to fundamental adhesion. The fundamental adhesion is described mathematically by the following equation:

The energy term here is expressed per unit area, thus, an increase in surface are can contribute to more fundamental adhesion. As explained in the section of wetting; Wenzel stated that increase in roughness enhance the wetting caused by the chemistry of the surface. Nevertheless, it is required that the wetting occurs homogenously without leading to the entrapment of air.

Therefore, surfaces, especially metal surfaces undergo an pretreatment like abrasion. Although the reason of a better adhesion cannot be said in general to be the rougher surfaces that is created by those pretreatments, there are clear examples that show this effect. An example of this are micro fibrous surfaces whereby through anodizing pores and whiskers on a nanometer-scale are created. The whiskers can be embedded in the adhesive while the adhesive can penetrate in the holes, in this way, there is a double interlocking effect. After the investigation of the locus of failure and analysis of the surface, it could also be concluded that microfibrous surfaces appear to increase the adhesion by increase in energy dissipation during fracture. Thus this shows that besides an enhancement in fundamental adhesion there is also an increase in energy dissipation during fracture that also contributes to the strength of adhesion.[22]

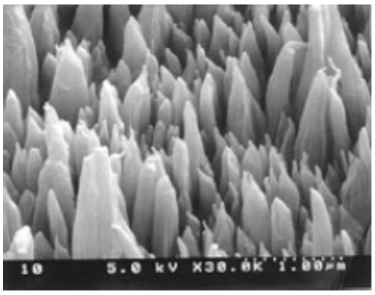

Figure 2.13: Scanning electron micrographs of microfibrous oxides on steel.[22]

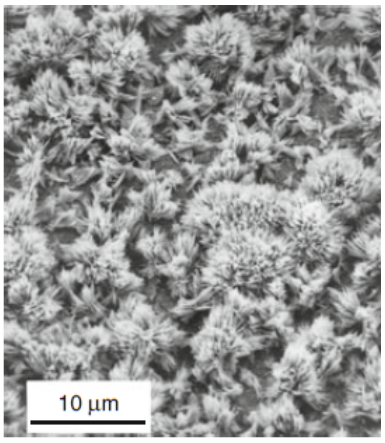

Figure 2.14: Scanning electron micrographs of microfibrous oxides on copper.[22]

In the case of polymer adsorption there is another approach to the effect of roughness, which is from the viewpoint of interaction potential energy. Different studies found that due to high entropic considerations, the polymers were favored to attach to the peaks while binding at the valleys is both due to entropic as well as enthalpic considerations. 3D-coil structure of the polymer is favored from an entropic view, therefore the entropic penalty associated with adhesion is reduced. In addition, more interaction is provided due to the surface curvature with as consequence more enthalpic gains. [22-27]

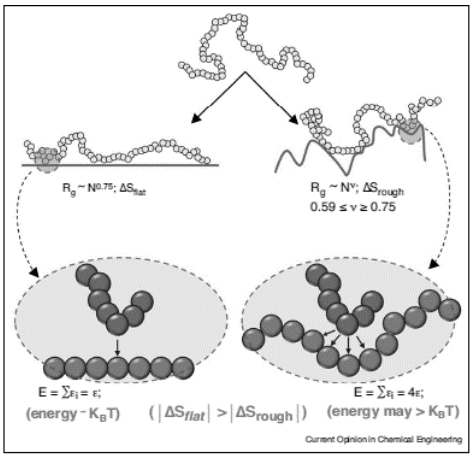

Figure 2.15: The 3D -coil structure is energetically more favorable than the 2D structure.Therefore, there is a reduction of the entropic penalty associated with adhesion. Moreover, there are more enthalpic gains(interaction between the molecules) due to the rougher surface (right bottom).[26]

2.4 Characterization of the mechanical behavior of encapsulants

2.4.1 Viscoelastic behavior of polymers

Rheology is the branch of physics that studies the flow of matter. In general it can be said that rheology studies the relationship between stress and deformation. This relationship will differ dependent on the state of matter, on one side there are fluids and on the other side there are solids. The behavior of fluids when deformation is applied is described as viscous behavior while solids show elastic behavior. Then you have materials that show characteristics of both, namely viscoelastic materials. Nearly all materials are viscoelastic. When a material is more viscous it is called liquid and if it is more elastic it is called a solid.

The rheological parameters that could be determined by rheological measurements are clarified with the two plate model. For Solid like materials the rheological parameter is the modulus. The shear stress divided by strain or amount of deformation is the modulus of the material. Flow, on the other hand, is a special case of deformation. In this case it is not the amount of deformation but the shear rate of deformation that is considered. The rheological parameter in this case is the viscosity of the material and is per definition the stress divided by the shear rate of deformation or the velocity of the fluid. Fluids show viscous behavior because of the internal friction due to the electrical cohesive forces between the molecules.

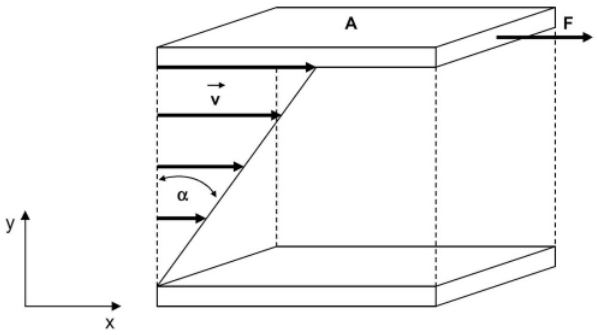

Figure 2.16: The two-plate model is used to describe the definition of rheological parameters[27]

Applying load to pure elastic material the deformation shows no phase lag (vice versa when deformation is applied). In the case of constant strain (or stress), when a step function is applied, the response will be a constant stress with a value according to the Hooke's Law;

$$\sigma = Ee \tag{2.7}$$

with E the elastic modulus, σ the sress and e the strain. If the excitation is a cyclic load, for linear elastic materials, the response will be strain in phase with the excitation and the law of Hooke's will still. Dynamic measurements are performed through applying the deformation in the form of a sine curve, the response will also be a sine curve without a phase lag. Thus, purely elastic materials do not dissipate energy while loaded and removed. Pure elastic solids will show a constant elastic modulus no matter the ambient conditions. Metals for example are considered as perfectly elastic material.

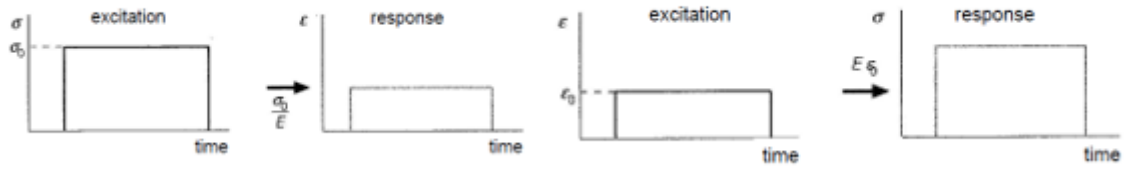

Figure 2.17: The response of a perfectly elastic material to a constant stress (left) and constant strain (right)[29]

In case of a purely viscous fluid, also called Newtonian fluid, when a constant load is applied, the response on this will be the strain in a linear equation. This is according to the Newton's law :

$$\sigma = \mu\epsilon \tag{2.8}$$

The derivative of the strain, the strain rate, is proportional to the stress with the proportionality factor the viscosity. As can be seen in fig. the strain remains after taking away the load. Similar to the pure elastic solids, purely viscous materials will show, at ambient constant conditions, the same viscosity no matter how they are stressed. When cyclic load is applied in the case of purely viscous material will ideally show a stress with the same sine curve but with a phase lag of 90 degrees.

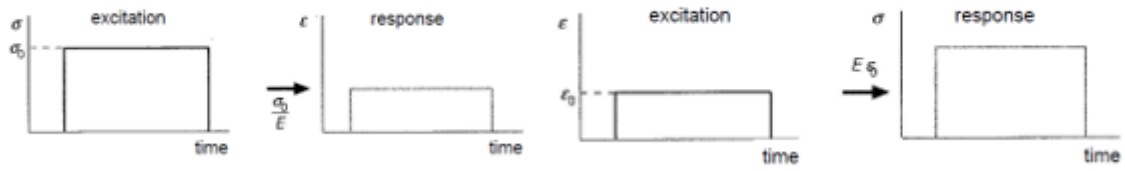

Figure 2.18: The response of a viscous material to a constant stress (left) and constant strain (right)[28]

Since viscoelastic materials exhibit both of the characteristics, when a cyclic load is applied the response will be sine curve with a phase lag between 0 and 90 degrees. Through the Viscous character these polymers show strain rate dependence on time while the elastic part causes stress in function of the deformation. The elastic component is more pronounced by faster movements and lower temperatures. In fig. The elastic portion and the viscous portion can be distinguished in the strain behavior when a constant load is applied.[28-30]

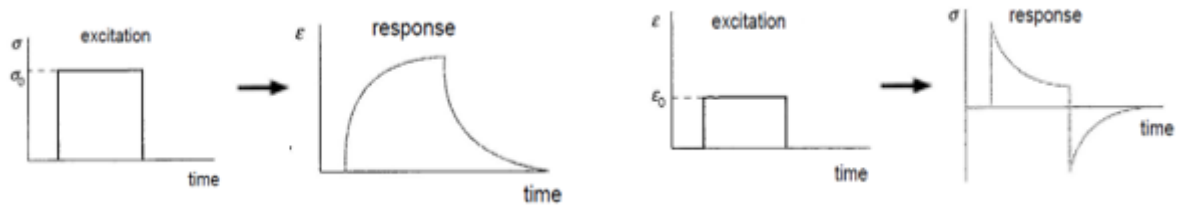

Figure 2.19: The response of a viscoelastic material to constant stress (left) and constant strain (right)[28]

2.4.2 Constitutive properties

There are different procedures to determine the mechanical properties of polymers. These are static, transient or dynamic testing. Static tests are perhaps the most common tests to determine the mechanical properties as the elastic modulus , shear modulus and the poison coefficient ν. However these tests are performed without taking into account the time dependency of the material. Viscoelastic materials, on the other hand, are materials that, as the name implies, show both viscous and elastic character. The Viscous character is the fluid-like behavior of the material and shows time dependency when stress is applied, while the elastic character is the solid-like behavior and is time-independent. Thus the static tests provide only information about the elastic part of the material.

The transient tests and dynamic tests, on the contrary, include the temperature and time dependency of the specimen and are performed to gain information about the longterm mechanical behavior. Transient tests are for determining the creep compliance D(t), axial or J(t) in shear. It is also possible to evaluate the time and temperature dependence of the material with dynamic tests. These tests measure the frequency and temperature dependence of the viscoelastic materials analogous to the transient tests. The parameters measured are the storage modulus E' or G' (g prime), loss modulus (E" or G") and the loss tangent. These parameters are frequency dependent. The frequency in dynamic tests qualitatively relates to the time dependency in the transient tests since w=1/t.

For static testing, a load is applied slowly to not have time dependency. A tensile test is a form of static testing, a bulk specimen is subjected to a slowly increasing load while the resulting load-deflection curve is recorded. These tests are easy to perform since the testing adhesives are bulk specimens, which means that also the deformation on the specimen is large and thus comfortable to measure. However, these tests are widely used and are useful to determine essential parameters as the modulus of elasticity , shear modulus and Poisson's ratio, ν.

Transient tests include creep and relaxation tests. Creep tests are performed by setting predefined stress and holding this constant during a period while the deformation is measured. Relaxation tests are performed similarly, but now the specimen is subjected to deformation while the stress is monitored. These tests are mostly conducted on simple-shape bars under uniaxial stress. Creep is the phenomenon that some materials, especially polymers, can deform permanently under constant stress, which is below the yield stress. The effect can be more severe if the temperatures are high and around melt temperature. The strain accumulated can even cause a rupture after a time. It is therefore important to know how the time and temperature influence the behavior of the material.

$$Stress(t)/strain = modulus E(t) \tag{2.9}$$

$$e/stress(t) = complianceD \tag{2.10}$$

It is important to note that the modulus and the compliance are not simply the inverse of each other, or at least not for viscoelastic materials. For perfectly elastic solids, this would be the case. The formal relationship between the compliance and the young's modulus is given by the following equation:

$$\int G(\tau)J(t-\tau)d\tau = t \tag{2.11}$$

Dynamic tests are conducted on bulk specimens in shear or in tension, while the specimen is subjected to either a sinusoidal stress or a sinusoidal strain. There are different techniques to perform dynamic tests. Oscillation tests can be performed for evaluating the viscoelasticity of a material and rotational tests can be conducted for viscosity measurements. The amplitude and the frequency of the sinusoidal stress or strain can be varied and the tests can be performed at different temperatures. Most common techniques are therefore; frequency sweeps whereby the frequency is varied while the temperature is held constant, and temperature sweeps whereby the frequency is constant and temperature is varied. Amplitude sweeps are performed mainly to determine the linear viscoelastic region (LVE) of the polymer. These tests are performed at constant frequency while the deflection, thus the amplitude of the sine, is increased step-wisely.

The dynamic mechanical properties that are measured by carrying out a DMA analysis, are the storage modulus, the loss modulus and the tan modulus. [32]

2.4.3 Time temperature equivalence

As earlier mentioned, it is important to characterize the long term behavior of polymers since the properties change with time and temperature. To do this transient or dynamic tests can be performed. However, every experimental work has its limits. These limits are in two ways, one are the limits of the measuring instrument, the other one is the time available. Since the goal of these experiments are determining long term behavior. This means that there is interest time periods of weeks, months and years. It speaks for itself that a real time experiment is not of the order. In such a dynamic testing measuring lower frequencies can take days or even weeks while to higher temperatures simply do not lie in the specs of the instruments.

Despite the limitations, it is possible to extent the time range to have a long time behavior. This is possible because polymers show time temperature equivalency. The time temperature superposition principle is based on the equivalent behavior of a polymer on higher temperature to a polymer at a lower temperature but at a greater time range or lower frequency. Or vice versa the same can be said for low temperatures and higher frequencies. Since the behavior is the same and there is mainly a constraint on the range of frequency, the range can be extended through measuring the sample within a broad range of temperature. In this way it is possible to extend a measurement performed over a range of 3 decades to 7 decades. Since the range of temperature for which the measurements can be done in is in theory generally going from -50 degrees to 600 degrees. Of course this is in theory and the material should not undergo any degradation during the measurement. Furthermore it is more convenient to have one single curve with one parameter at once rather than have a function dependent on two parameters. In this way the two variables time and temperature can be separated an it is easier to understand the rheological behavior at different conditions.

This relationship of the modulus at the reference temperature and time to the modulus at an arbitrarily chosen temperature is mathematically described by the following equation.

$$E(T_1, t) = E(T_2, \frac{t}{a_t}) \cdot \frac{\rho(T_1)T_1}{\rho(T_2)T_2} \tag{2.12}$$

$$b_t = \frac{\rho(T_1)T_1}{\rho(T_2)T_2} \tag{2.13}$$

The first factor in this equations represents the horizontally shift with at the shift factor and rho the density. The second factor is the vertically shift, this one represents the vertically shift also represented as bt. This one is actually a correction factor to the change of modulus with temperature. The vertically shift factor but will only change slightly when compared to the large changes due to the horizontally shift factor. Therefore in most cases this factor can be neglected.

Williams Landel and Ferry found that the change of shift factor with temperature, followed the same relationship generally around the glass transition temperature. Thus an equation is found for the shift factor around Tg

$$Loga_t = \frac{-C_1(T - T_g}{C_2 + T - T_g} \tag{2.14}$$

C1 and C2 are constants an Tg the glass transition temperature.

As WLF is valid only around Tg, another equation is needed to determine at temperatures outside this range. Here the Arrhenius can be used;

The extending of the frequency range by making use of the time temperature superposition principle is done through shifting the curves measured at another temperature than the reference temperature, to the reference temperature itself. After the shift factors are determined, they can be fitted to one the two mathematical models; The Arrhenius model or the Williams-Landel-Farrel model. Hence, the material constants are determined and the time temperature shifting can now be done for a randomly temperature or time.

2.4.4 Master curve

The shifting is done by the software. First a reference temperature is chosen. To shift the curves measured at different temperatures to the reference temperature a overlap window is determined. This done by determining the distance between the two curves and minimalizing it by using the method of least squares. Subsequently the best fit is used to shift the curve measured on the next temperature. The same process is used each time. When all the curves are shifted, the mastercurve is constructed. Now the master curve is fitted, te

$$Loga_t(T) = log(t(T) - log(t'(T_R)) \tag{2.15}$$

With t' the shifted curve.

Williams-lander-ferry have shown that for thermo rheologically simple materials always the relation for the shift factor was the following for all materials. There are two material dependent constants in these equation. When these are known, the shift factor can be determined and the conversion of time to temperature is made easily.

However, this equation is valid only under certain conditions. The material should be simple, this implies a amorphous material. Also this equation is only valid around the Tg to 100 degree celcius plus Tg. Beyond this range another more general equation is used, namely the Arrhenius.

Chapter 3

Study of the surface profile in adhesion

3.1 Introduction

Roughness influences adhesion significantly. Different studies dealt with the relationship of roughness to adhesion, mostly theoretically but also practically. It is commonly agreed that average roughness alone is not sufficient to understand the contribution of the surface topology to the adhesion strength. In [], the authors studied the effect of substrate roughness on adhesive joints through the complete characterization of the surface. They have generated different levels of roughness through abrasion and impression processes to evaluate roughness dependency. The influence on the joint strength is determined through lap shear tests. They have found that higher surface roughness led to a proportional increase of the joint strength until it reached a maximum. A further increase of the surface roughness almost did not affect or slightly decreased the joint strength. They ascribed this critical value of roughness to the change of summit density Sds of the surface topography. Therefore, it has been concluded that surface roughness effect depended strongly on the detailed characteristics of the surface roughness. [] However, it should be noted that they did not consider the surface roughness on different length scales

The objective here is the characterization of the surface profile of two types of adherends.The two types of adhesives are screenprinted Ag-surface and a sreenprinted Al-surface. These are the materials that are commonly used in the PV-industry.Ag-contacts are used for the front side metallization of the solar cells, while the Al-contacts are used for the rear metallization of the solar cell.

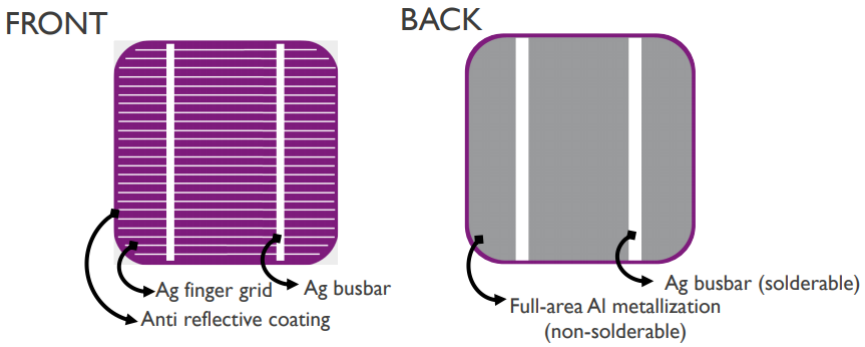

Figure 3.1: The response of an perfectly viscous material to constant stress (left) and constant strain (right)

The complete morphology will be determined by a variety of statistical descriptors as parameters of height, wavelength and shape of the surface. Furthermore, different length scales will be considered in the description of the surface topology.

3.2 Materials and Methods

Confocal Laser Scanning Microscopy

The principle of working of a Confocal Laser Scanning Microscope is based on the working of a conventional optical microscope,but provides higher optical resolution by masking the out-of-focus light. This works as follow: a beam of light is passed on a very small apparature which illuminates a small spot on the sample. The same small spot is detected on the same time by the detector because the reflected beam is getting trough a equally small apparature. If the point is perfectly in focus the light can pass and fall on the CCD camera otherwise it will be physically masked (by the multi-pinhole disc). The working princple is illustrated in figure 5.2 During the measurement the sample is moved in the height (z-direction) through the different focal planes, see figure 4.3.0.3. So the unfocussed details are filtered out and thus the confocal microscope is capable of high resolution in the nanometer range. The images are horizontal slices through the topography of the sample. The software constructs with the differen confocal images an exact three-dimensional image.

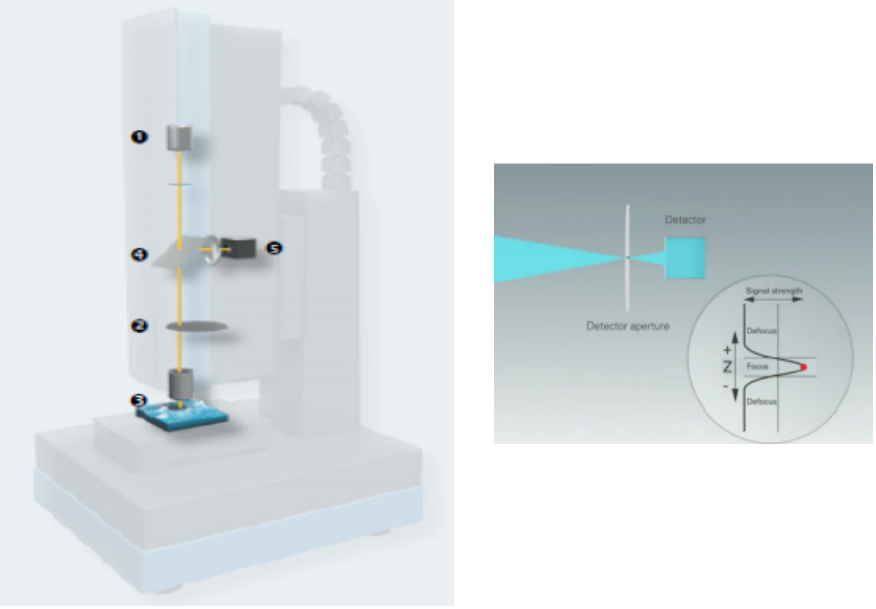

Figure 3.2: working princple of a Confocal Laser Scanning Microscope, only the plane in focus will reach the detector

Statistical Roughness and Surface roughness parameters

Roughness parameters

The roughness values used for the project are shown in this summary accompanied with a short definition. The roughness values are defined in EN ISO 4287.

- **Rz**: the sum of the largest peak and the highest valley in the measured profile.

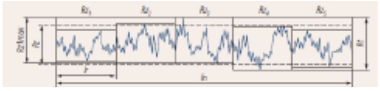

Figure 3.3: Mean roughness depth Rz

- **Rp**: Maximum peak value
- **Rv**: Maximum valley value

  The Rp and the Rv visually shown on the picture below.

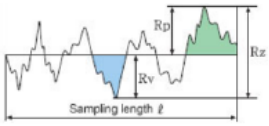

Figure 3.4: Peak and valley roughness Rv and Rp

- **Ra**: arithmetic average of the absolute values of the roughness profile ordinates. The Ra value is defined on the drawing of the tube (Figure 1).

$$R_a = \frac{1}{l} \int_0^l \mid Z(x) \mid dx \tag{3.1}$$

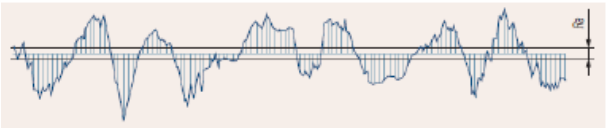

Figure 3.5: Arithmetical mean roughness value Ra

- **RSm**: Mean value for profile width. RSm is the mean value of the spacing Xs_i of the profile elements shown in the figure below.

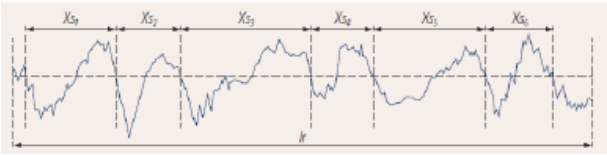

Figure 3.6: RSm value

Surface roughness parameters

Summary of the statistical surface parameters			
Parameters		Description	Possible Values
Sa	Average roughness	Arithmetical mean deviation	Any
Sp	Maximum peak height	The height of the highest peak within the defined area	Any
Sz	Ten-point height	Average height of 5 maximum and 5 minimum	Any
Ssk	Surface skewness	Asymmetry of the height histogram	Ssk = 0: symmetric distribution Ssk <0: bearing surface with holes Ssk >0: flat surface with peaks Ssk >1: extreme peaks or holes
Sku	Surface kurtosis	Sharpness of peaks and valleys of the surface topography	Sku ∼3: Gaussian distribution Sku <3: broad height distribution Sku >3: narrow height distribution
Stdi	Texture direction index	Preferential direction	Stdi ∼0: very dominant direction Stdi ∼1: no dominant direction

3.3 Results

3.3.0.1 results surface roughness

Surface Roughness
Al(x150)

	Sa	Sz	Ssk	Sku	Sp	Std
Av.	0.802	12.849	-0.185	7.268	6.205	72.498
Min	0.623	8.916	-2.167	3.547	3.370	0.000
Max	1.064	24.055	2.952	32.376	14.592	180.000
Dev.	0.0873	2.753	1.107	4.732	2.232	49.995

Multi-Line Roughness
Al (x150)

	Ra	Rz	Rsm	Rp	Rv
Av.	0.756	5.803	18.428	2.644	3.159
Min	0.581	4.535	12.112	1.811	2.541
Max	1.043	8.673	35.342	4.336	4.464
Dev.	0.100	0.742	3.888	0.580	0.358

Surface Roughness
Ag (x50)

	Sa	Sz	Ssk	Sku	Sp	Std
Av.	2.699	34.213	-0.536	4.614	15.467	89.975
Min	2.523	31.081	-0.887	3.926	13.359	0.000
Max	3.204	38.318	-0.178	5.565	17.887	180.000
Dev.	0.210	2.292	0.225	0.583	1.393	89.975

3.3.0.2 3D surface profile

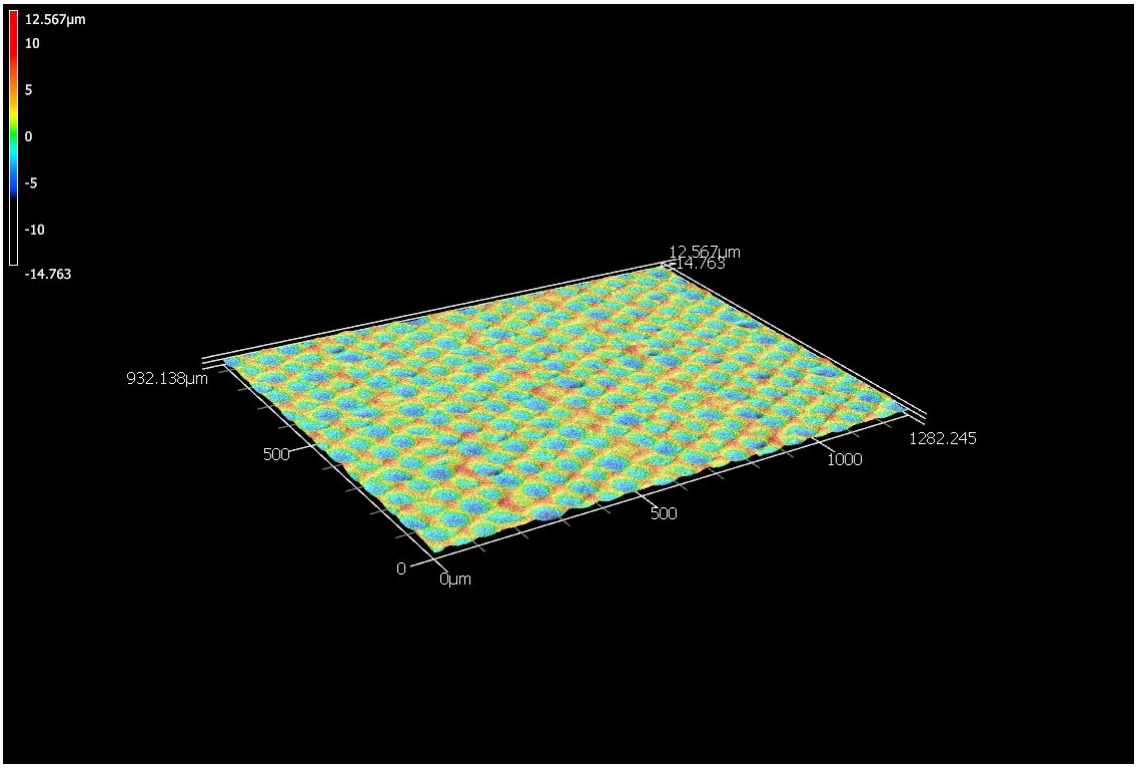

Figure 3.7: 3d surface profile of Ag-subtrate with magnification x50

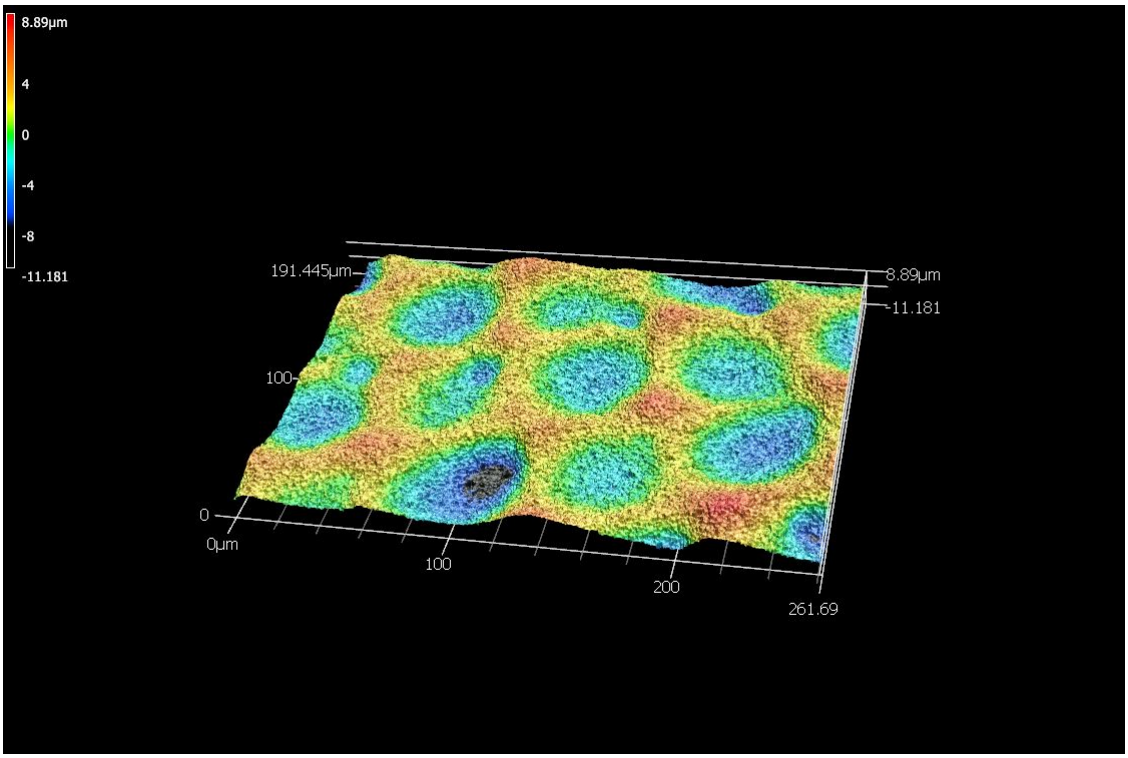

Figure 3.8: 3d surface profile of Ag-subtrate with magnification x150

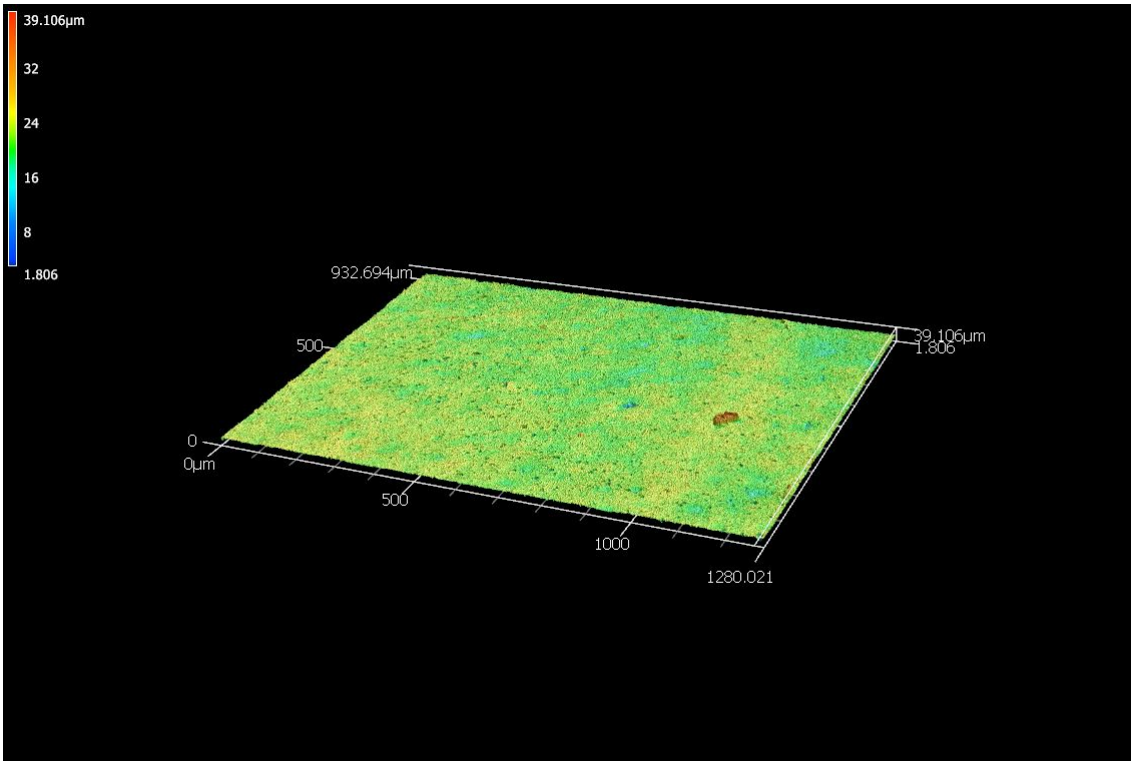

Figure 3.9: 3d surface profile of Al-subtrate with magnification x50

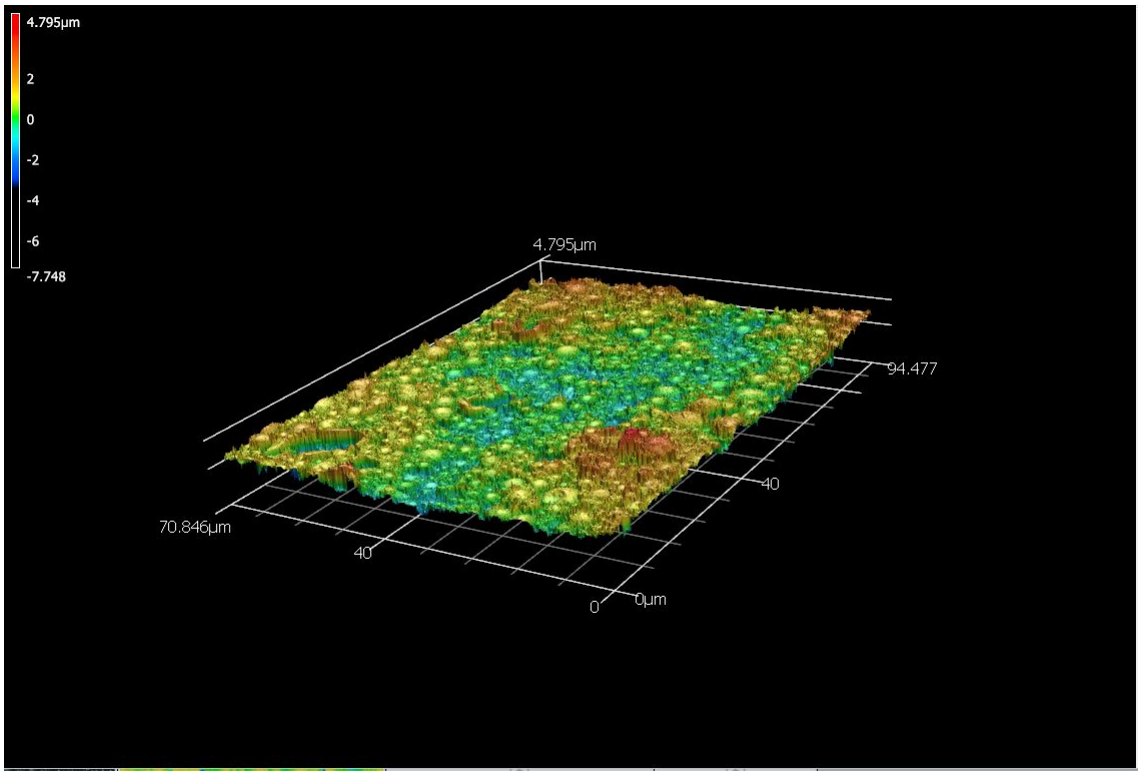

Figure 3.10: 3d surface profile of Al-subtrate with magnification x150

The two substrate appear to have quite a different surface morphology. The Al-substrate show different roughness profile at larger length scale compared to the lower. At the larger length scale it has a quite smooth surface profile, while at lower length scale it shows a more random distributed roughness profile. It has some cavities as well as bowl-shaped aspirities. The Ag-substrate on the other hand, has a rougher surface at larger length scale, compared to the Al-surface. However, at lower length scale has it a very smooth surface.

Chapter 4

Study of the mechanical behavior of the encapsulant in adhesion

4.1 Introduction

One of the degradation mechanisms that causes delamination is as discussed in the section of 'degradation mechanisms', the residual thermal stress in the PV-modules. The accumulation of internal stress in the module components starts at the lamination process. Cooling the module down to room-temperature from temperatures around 150 degrees Celsius causes bending of the components due to different coefficients of thermal expansion (CTE) for the different components. (Fig.)This mismatch in CTE-coefficient is also experienced during the operation of the PV-module, as the temperature changes cause external stress. Although the residual stress in the laminates do not cause directly significant cell cracking, the superposing of the residual thermal stress after lamination to external thermal stresses can lead to regions of crack localization which can lead to the initiation of delamination and performance loss.[1][2]

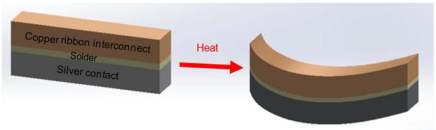

Figure 4.1: The effect of CTE mismatch of different materials on the metal contacts.

The factors that lead to delamination are extensively studied, most studies have treated the residual stress that is caused by the solder and lamination processes. However, recent studies demonstrate that the mechanical properties of the encapsulant have a significant influence on the deformation and the stress of a PV-module. The encapsulant was not expected to affect this behavior in the first place because of its low E modulus. Fig. Illustrates the components of the PV-module with respectively their E -modulus schematically. As can be seen, the E modulus is approximately 4 factors lower than the E modulus of the Si-cell.
In addition, the time and temperature-dependent behavior of the encapsulant also affects the long term behavior of the PV-module. Large scale tests to determine longterm behavior are very time consuming and expensive. Therefore, finite element simulations can demonstrate the long-term behavior on the PV-module level, once the long-term behavior of the encapsulant is determined. As in the section of 'mechanical behavior of the encapsulant', is explained, there are different techniques to determine these properties. Here, Dynamic mechanical analysis are carried out to determine the mechanical bulk behavior of the encapsulant.

4.2 Material and methods

4.2.0.1 Dynamic mechanical analyzer

Principle of working

The technique of dynamic testing with a dynamic mechanical analyzer is used to determine the storage, loss and tan moduli of the encapsulant. The instrument that is used to perform these tests is the Anton Paar MCR102. Fig.

Figure 4.2: Anton Paar rheometer of type MCR102 with additional a temperature chamber (left) and the plate-plate measuring geometry (right)

There are two sorts of DMA, a strain controlled DMA and a force controlled DMA. The dynamic mechanical analyzer can measure three things which are the angular deformation or the change of angular deformation by time (angular velocity) and torque. These raw data can then be transferred to a material quantity as stress or strain. These are the machine parameters. To calculate the other parameters, depends on the geometry and the dimension of the sample. Eg parallel plate / cone and plate, diameter 50 mm or 8mm.

Strain controlled

In this case, the transducer and the motor are separate. The sample is subjected to deformation via a motor. The transducer on the other hand measures the transferred torque. In fact it measure the force needed to hold the upper plate in place.

The strain controlled DMA sets a predefined displacement or amount of deformation mostly in a sine wave cycle at a defined frequency. A servo motor can control strain, strain rate and frequency. Subsequently the force needed for that displacement can be monitored by a transducer. The transducer measures the torque transmitted through the sample needed to hold the plate on which it is set in the place.

Stress controlled

On the other hand, the force controlled DMA applies a preset force on the sample at a specified frequency. The force needed is calculated to the torque as the motor can provide this in this manner. The displacement can be measured through a linear optical encoder or the typical LVDT technology.

Machine parameters

The rheometer or the dynamic mechanical analyzer can provide information about the viscosity of the material, viscoelastic properties or the transient response (usually a unidirectional test, creep response relaxation response)

To determine these rheological parameters there are only 3 machine parameters that are used. These are :

- Torque(N m)
- Angular displacement (rad)
- Angular velocity(rad/s)

Relating machine parameters to material parameters Calculated parameters, which are:

- Stress(Pa)
- strain()
- strain rate(1/s)
- viscosity)(Pa s)
- Modulus (Pa)

The material parameters range of use are referred in the specs of the machine. In order to have reliable results, the range in which the work is done should be in the range of specs.

With K geometry dependent factor. These factors are dependent to the geometry that is used and to the dimensions to the geometry. In this manner the machine parameters are related to the material parameters. In case of the plate geometry that is used the factor is.

The technique that is used to characterize the sample is the frequency sweep whereby the frequency is varied from 10 to 100s, while the temperature is held constant. These tests are conducted in the Linear viscoelastic region; the viscoelastic character can then be described with the Hooke's law for linear elastic behavior and Newton's law for the linear viscous behavior.

4.2.0.2 Procedure

Sample preparation

There are three types of an encapsulant, the most commonly used ones, that are characterized by the rheometer. These are two polyolefin(POE)- based encapsulants, Borealis and Arkema, and one EthylVenylAcetate (EVA)-type of encapsulant. The DMA-measurements are very sensitive to moisture and entrapped gases, therefore, the encapsulant samples are first put in the vacuum-oven to minimize those effects on the results. Subsequently, the encapsulant is laminated with the standard lamination process to which the PV-modules are subjected. The encapsulant samples are circular with a diameter of 50 millimeters and the thickness is approximately around 485 micrometers.

The dynamic mechanical analyses are conducted using a plate-plate geometry. This geometry is mostly used when performing frequency sweeps with soft solids. One disadvantage of this geometry is that the deformation speed is not constant over the entire plate gap; thus, the shear rate distribution depends on the radius. The value obtained conducting this measurement is the shear rate at the outer edge. However, in the case of determining the moduli of the polymer in the LVE-range is this of low relevance.[] The dimension of the used plate is a diameter of 50 mm, fig.

Linear Viscoelastic range

Amplitude sweeps are conducted first to determine the LVE range. These tests are conducted at variable amplitudes while keeping the frequency constant. It is possible to conduct this test in either the controlled strain mode or the controlled stress mode. In this case, the strain sweep, thus controlled strain mode, is performed. The frequency is held constant at 1 Hz while the strain is varied from 0,01 to 100 %.

Measurement test definition for Frequency sweeps

Different frequency sweeps are carried out at temperatures varying from 10 to 180 degrees Celcius. The measurement procedure for a single frequency sweep at a constant temperature.

- **Time Settings**:
  - 16 data points
  - No point duration setting
- **Measuring Profile**:
  Shear strain (oscillating)
  - Amplitude gamma = 0,15 %
  - Angular Frequency omega = 100...0,6 rad/s (logarithmic)

  Normal Force
  - $F_N = 8N$

4.3 Results

4.3.0.1 Process parameters

First the influence of the normal force and aspect ratio is determined by testing different samples of the same encapsulant that were prepared at the same time. However, after the first measurements the variation on the results of these samples were too large. The samples were measured at the same temperature, thus this large spread was not expected. The influence of the different factors that could have an impact is examined, as aspect ratio and the normal force. The reason appeared to be that the sample had to be heated up to form a melt. When the sample was first not melted, it did not make perfect contact to the plates, which resulted in different results each time a measurement was carried out.

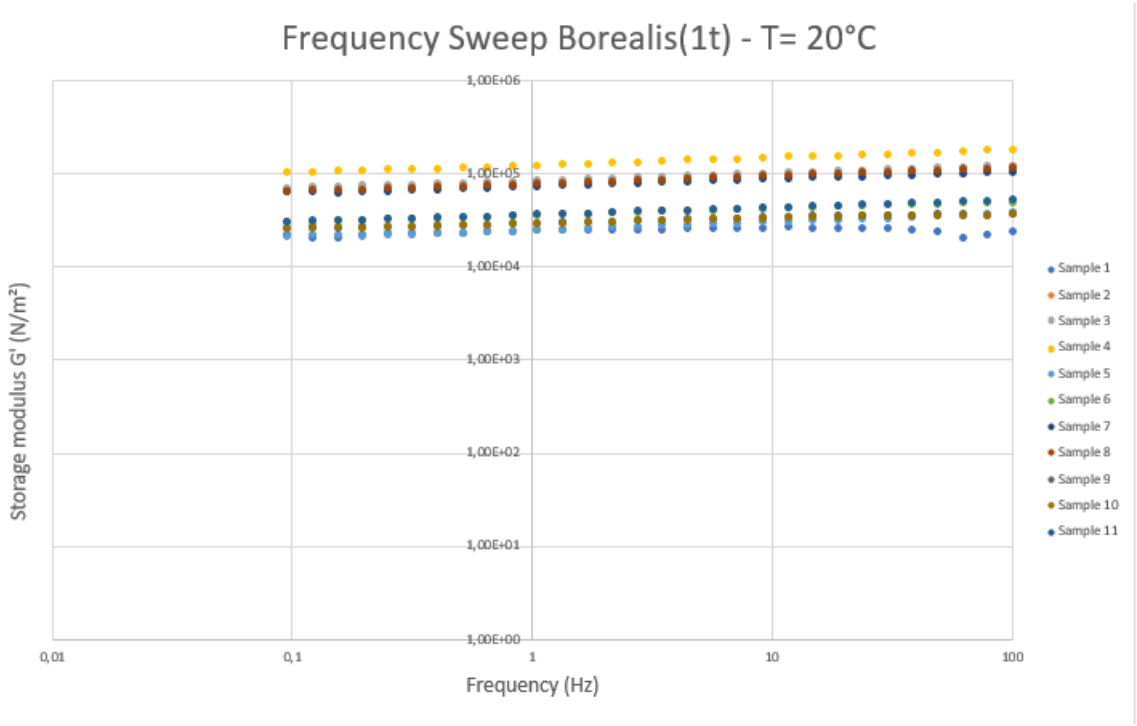

Figure 4.3: Storage modulus versus frequency curves for encapsulant Borealis dependent on the temperature behavior

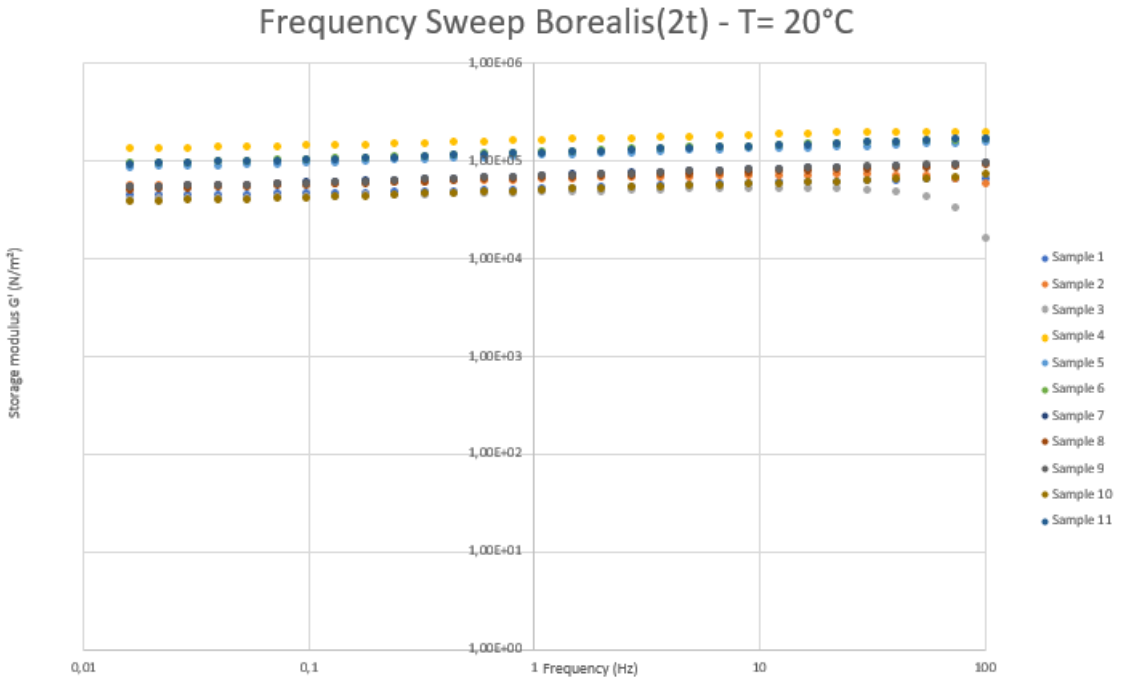

Figure 4.4: Storage modulus versus frequency curves for encapsulant Borealis dependent on the temperature behavior

4.3.0.2 The influence of aspect ratio on the mechanical properties

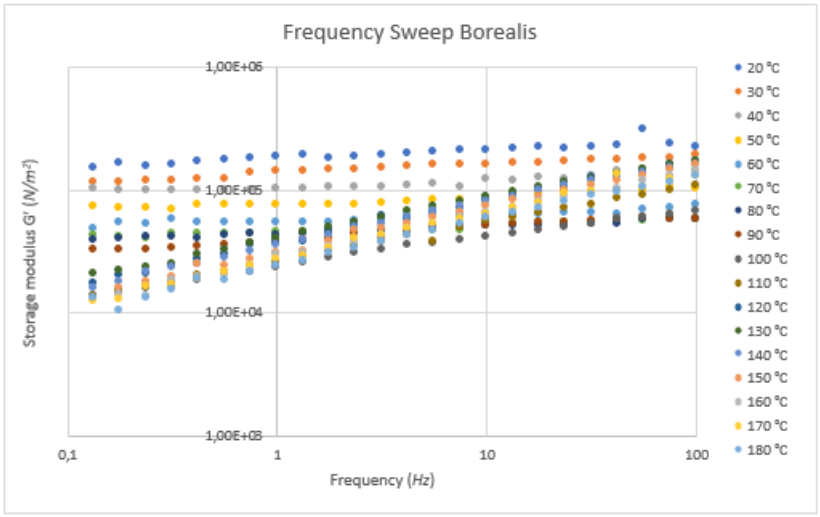

Figure 4.5: Storage modulus versus frequency curves for encapsulant Borealis dependent on the temperature behavior

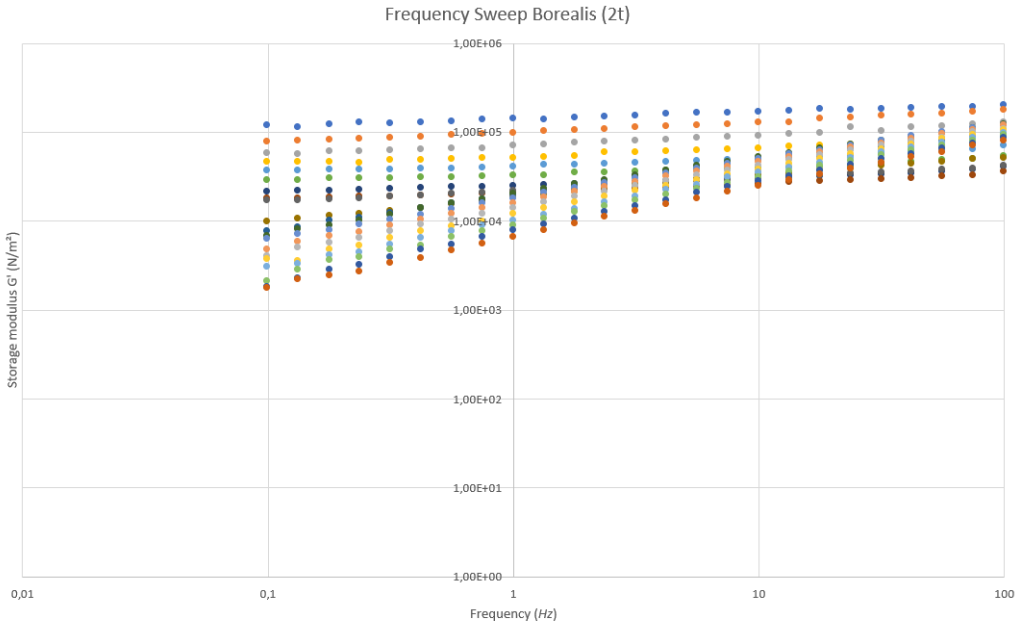

Figure 4.6: Storage modulus versus frequency curves for encapsulant Borealis dependent on the temperature behavior

The influence of the thickness of samples is evaluated. The first graph shows the results of one layer of encapsulant thickness, while the second graph is that of 2 layers thick encapsulant. However, it should be noted that the thickness is slightly less as the double after the lamination process.

4.3.0.3 Frequency Sweeps

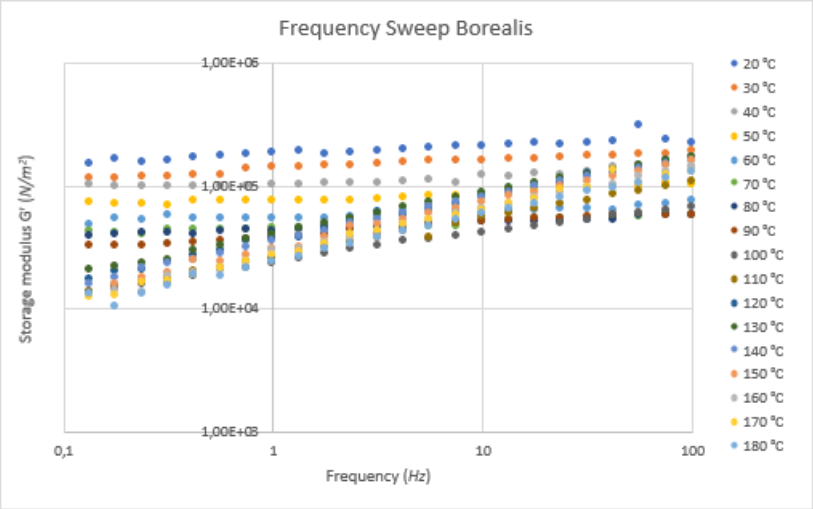

Figure 4.7: Storage modulus versus frequency curves for encapsulant Borealis dependent on the temperature behavior

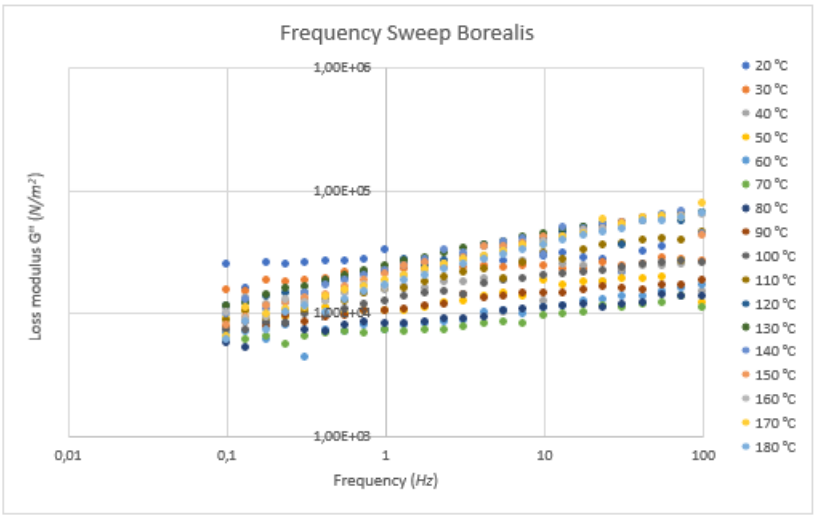

Figure 4.8: Loss modulus versus frequency curves for encapsulant Borealis dependent on the temperature behavior

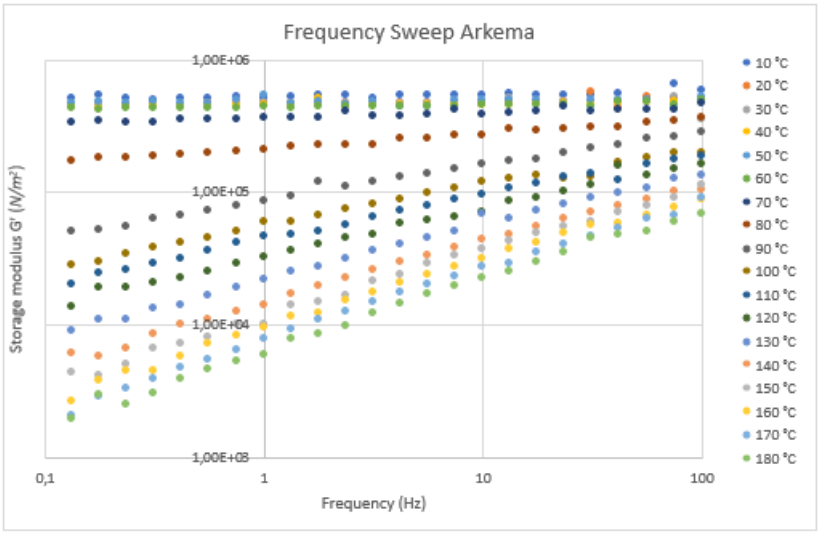

Figure 4.9: Storage modulus versus frequency curves for encapsulant Borealis dependent on the temperature behavior

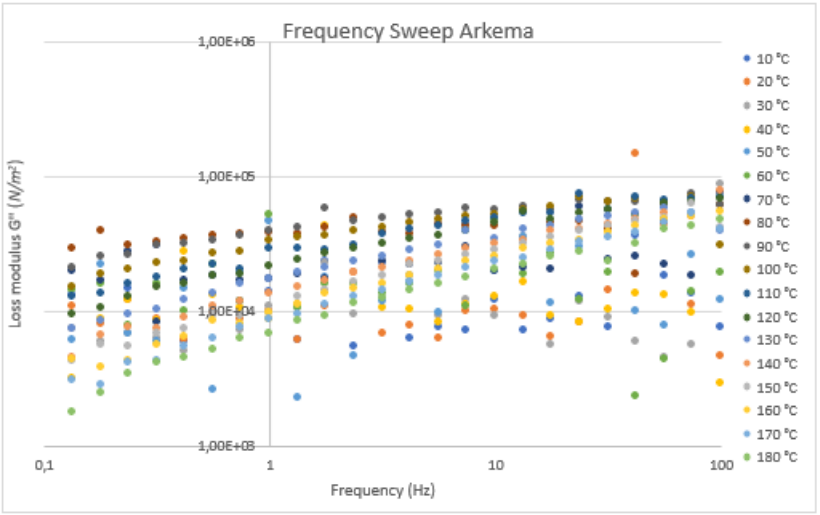

Figure 4.10: Loss modulus versus frequency curves for encapsulant Borealis dependent on the temperature behavior

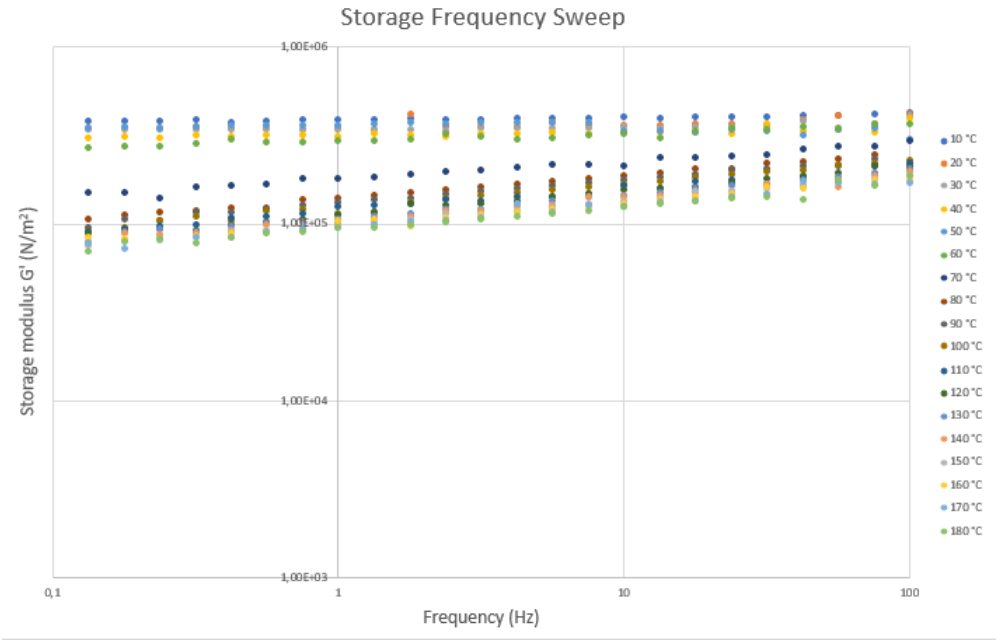

Figure 4.11: Storage modulus versus frequency curves for encapsulant EVA dependent on the temperature behavior

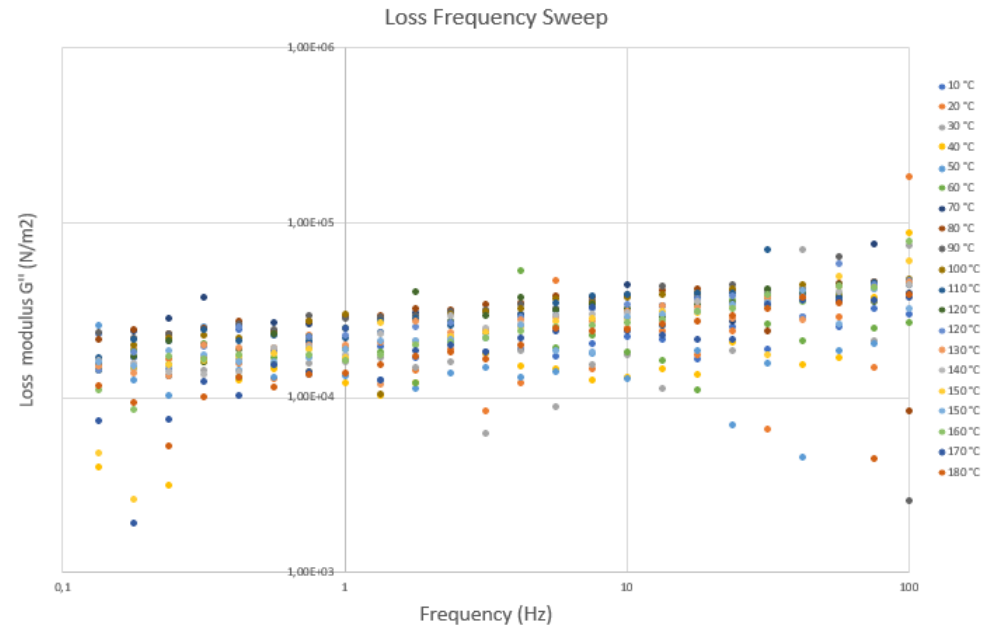

Figure 4.12: Storage modulus versus frequency curves for encapsulant EVA dependent on the temperature behavior

4.3.0.4 Temperature Sweep

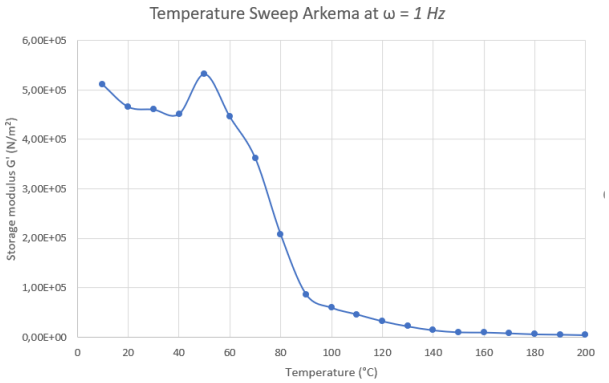

Figure 4.13: The response of an perfectly viscous material to constant stress (left) and constant strain (right)

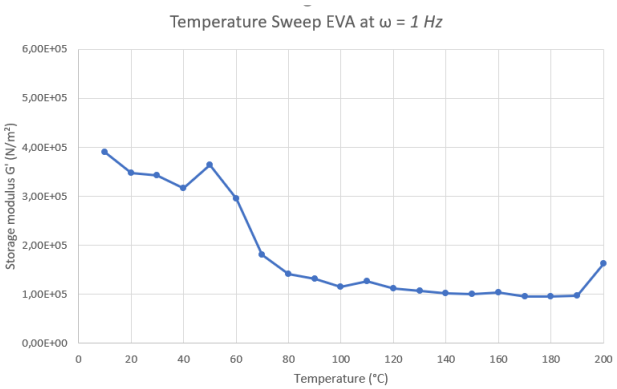

Figure 4.14: The response of an perfectly viscous material to constant stress (left) and constant strain (right)

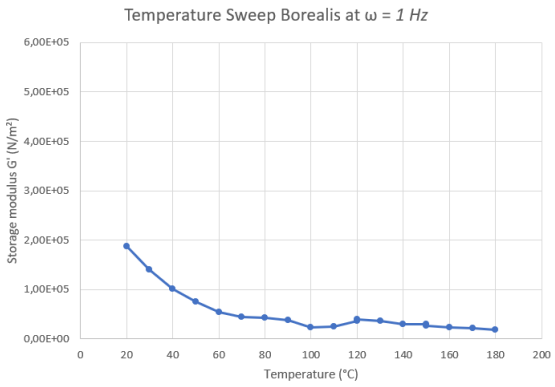

Figure 4.15: The response of an perfectly viscous material to constant stress (left) and constant strain (right)

Chapter 5

Study of the interface morphology: influence of process parameters materials

5.1 Introduction

There are different sorts of encapsulants that are used in the industry of photovoltaic. As already earlier mentioned, these materials should meet some requirements. Mostly not all the requirements could be achieved but an optimum should be chosen. The materials that are mostly used in the PV-technology are EVA (Ehtylene Vinyl Ace-tate)-based encapsulants and POE (Polyolefin elastomer) encapsulants.[] The adhesion between the encapsulant and the metallization is a focus of interest in this case. To characterize this, a replica laminate is going to be made. Subsequently, this can be examined to have more insight in the adhesion mechanisms that occur in the interface.

The lamination process of the encapsulant is known to influence the quality of the PV-module. In the section of adhesion strength, it is discussed that the mechanical properties and viscosity of the adhesive play a major role in the penetration of it in the substrate. Process parameters of the lamination process, namely the temperature and the pressure, will influence the viscosity of the adhesive. Therefore, the influence of these different parameters will be checked on the bonding which will be formed during the lamination process. Similarly, it is also discussed that the morphology of the substrate influences the bond formation as well. Therefore, combinations of three commonly used encapsulants and two sorts of metallization will be processed at different lamination conditions, to see if it affects the bond formation at the interface.

Further, it is also well known that the daily thermal cycles to which the PV-modules are subjected, are the main reason why degradation is experienced. The difference in CTE coefficient of the bonded materials arises internal stress in the laminates. [] Thus the internal stresses considered due to this, the elastic properties of the encapsulants are of significance. This effect is not studied in the early literature, which is probably due to the low elastic modulus of the encapsulant that was not expected to contribute to the internal stress in a PV-module. However, it is showed that different encapsulants with different elastic modulus make a significant difference in the residual stress of the modules.

5.2 Materials and method

Sample layup

To have an insight in the influence of the enumerated parameters there are made samples. A layup is made of the same layers as present in a standard PV-module. Cross sections are made of these mini-laminates (3cm x 3 cm) to subsequently examine these with a Scanning electron microscope. In this way the it is possible to see the interface at closer magnifications and have an insight in the possible adhesion mechanisms. Each layup existed out of 3 different encapsulants and for each encapsulant, there are two sort of metallization that is used, Ag paste coating and Al paste coating. These are the same samples as used for the surface characterization in section. This resulted in a set of 6 laminates, the different layers are illustrated in fig..

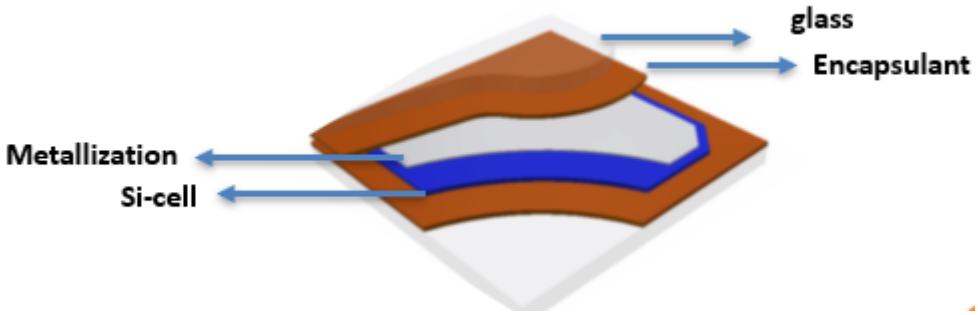

Figure 5.1: The different layers of the layup

The lamination process

The lamination of the different layers of a the PV-stack takes place in a laminator. This machine exists out of two chambers, the upper chamber and the lower chamber wherein the pressure can be controlled properly as well as the temperature of the hot plates. Three main steps can be distinguished in the lamination process, the preheating , pressing and as last the cooling step. During the preheating step, vacuum is applied to both the lower chamber and the upper chamber to 1mbar. During this step all the air is evacuated to prevent air bubbles in the lamination stack. While evacuating the air in the two chambers, the upper and lower plates are heated simultaneously, doing so the moisture is removed too. The plates are heated to a rate of 5 degrees / min to prevent glass warping. It is reported that applying temperature differences abruptly to glass causes it to get curved [IEA]. For this reason, there are also metal pins provided to prevent direct contact of the PV-stack with the hot plates. The temperature needs to be maintained around the softening point of the encapsulant so that its melts and behaves as an adhesive. After this step the pressing step takes place. While the lower chamber is still vacuum, a relative higher pressure which is still in vacuum, is applied. This realizes the pressing step with the membrane of the upper chamber. While doing this the temperature is held constant. The duration of this step is especially of importance when the adhesive is curing.

Sample prepartion for the SEM

After the lamination of the PV-modules, cross-section are made to examine the interface with SEM. Before taking the cross-sections to be able to examine the interface with the SEM, the samples underwent some preparation steps. First, the samples are embedded in epoxy resin which should serve as support for the samples. The support of the epoxy resin is also needed before the samples are cut, otherwise it is possible to damage the samples. Afterwards to produce a flat surface, the samples are grinded and polished. Since the metallic components are able to conduct the electrons in the SEM, no further preparation for this part would be needed. The encapsulant

on the other hand, is non-conductive and needs a thin layer of conducting graphite of 1 or 2 atoms layer thickness to be spread over it to visualize it by SEM. However, not being conductive causes a charging effect of the encapsulants, whereby this can be used to enhance the contrast between the metallization layer and the encapsulant in the interface.

5.3 Results

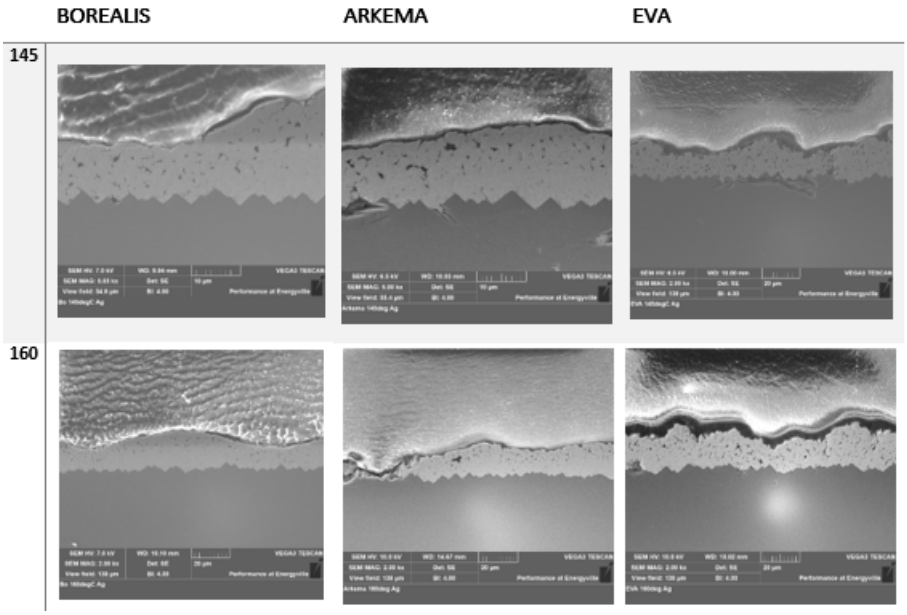

Figure 5.2: Ag-substrate

The surface roughness at large length scale of the Ag-strate appears to influence the bond forming significantly. There are some cavities that seem to be an effect of contact angle hysteresis (discussed in section 2.3.2). The EVA seems to adhere most loosely, while it is the most viscous encapsulant of them all. The reason is probably the higher stifness of the encapsulant.

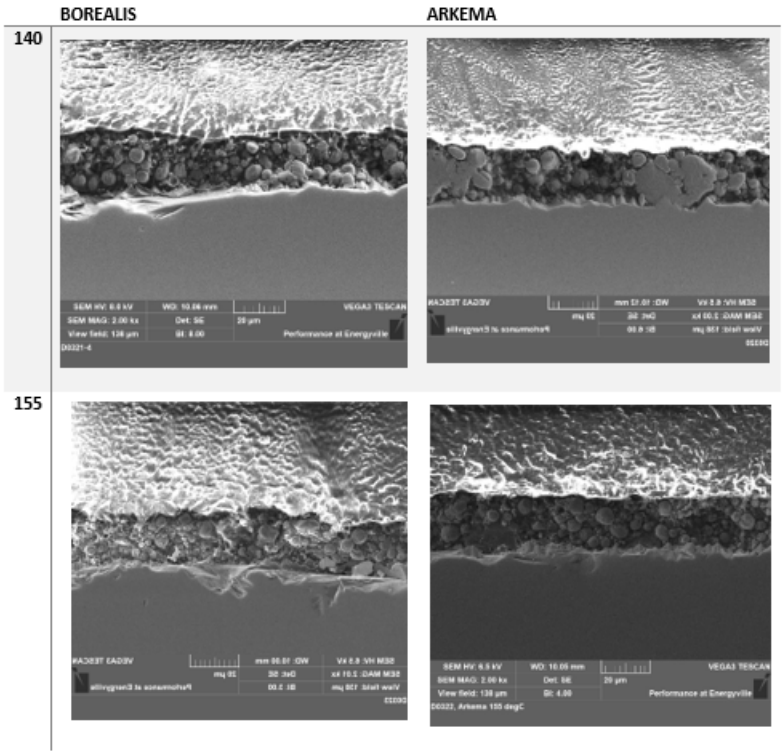

Figure 5.3: Al-subtrate

On the contrary,the Al-substrates seems to make good contact to the substrate. Indeed, the Al-substrate has a quite smooth surface roughness at larger length scale, as it was found in the study of the surface profile. This seems to affect significantly, despite the rougher surface roughness at lower length scale.In addition, it can be seen that even can penetrate in the cavities. This enhances the interlocking effect.

Chapter 6

Conclusions

The most prevalent degradation mode of PV-modules in the field is delamination. Delamination can occur between different components in the laminate. However, it is reported to happen mostly, selectively around the metallization, as discussed. Therefore, the objective of this master thesis is to characterize the bulk and interface behavior of encapsulants. The surface finish of joining parts is very crucial since the properties of the surface control the way it interacts with its environment. Therefore, the analysis of the surface is of great importance for studies of adhesive bonding. The surface profile of the adherend influences the adhesive bonding in different ways, as discussed. It has a significant role in the wetting phenomena, which is of great importance regarding the fundamental adhesion. In the case of polymer-metal interaction, the interlocking effect plays a crucial role in the adhesion bond. Therefore, surface characterization of the Ag-substrate and Al-substrate is carried out.

Different statistical descriptors of the surface thoroughly characterize those surfaces. Furthermore, different length scales are considered in these measurements. The obtained results can be used in future work to correlate the adhesion strength to the roughness. As follow, the bulk behavior of the encapsulant is studied. In order to have excellent adhesion, intimate contact is required; the rheological parameters influence the wetting behavior. The viscosity of the adhesive influences the penetration of the adhesive in de adherend to form a bond. The more viscous the encapsulant, the more it can penetrate in the adherend. Similarly, the stiffness of the encapsulants influences the residual stress in the laminates after the lamination process. Besides the initial bond strength, the mechanical properties determine the long-term behavior of the joint. The encapsulants show viscoelastic behavior and therefore are time and temperature-dependent. Dynamic mechanical analysis is carried out to evaluate the mechanical properties of the encapsulant in function of time and temperature. These results can be used to fit a material model to the master-curve that can be obtained with these results (discussed in.) which is an input of the reliability simulation models.

Finally, the interface is investigated using cross-sections that are examined with the SEM. In this way, it was possible to get more insight into the influence of materials and process parameters. The temperature of the lamination process seems not to have a significant effect on the penetration of the adhesive in the adherend. Also, the viscosity of the encapsulants does not seem to affect the interface in a noticeable way, while the viscosity of the adhesives is quite different as the measurements show. However, the substrate and thus the surface profile of the metal appears, as expected, to affect the wetting significantly and thus affecting the interface. The study of the surface profile has shown that the Ag-substrate is significantly rougher compared to the Al-surface. The effect of this can be seen in the results of the SEM-images, as the adhesive seem to make more intimate contact with the Al-surface. Besides, the roughness of the Ag-surface at a larger length scale also seems to alter the contact angle of the wetting and cause hysteresis (as discussed.). Thus, the roughness at the larger length scale seems to affect the bond formation significantly.

Bibliography

[1] "Energyville" [Online]. Available: https://www.energyville.be/.

[2] "University Hasselt, "IMO - IMOMEC," Accessed February 20th 2015. [Online]. Available: http://www.uhasselt.be/IMO

[3] M. C. C. de Oliveira, A. S. A. Diniz Cardoso, M. M. Viana, and V. de F. C. Lins, "The causes and effects of degradation of encapsulant ethylene vinyl acetate copolymer (EVA) in crystalline silicon photovoltaic modules: A review," *Renew. Sustain. Energy Rev.*, vol. 81, no. March 2017, pp. 2299–2317, 2018.

[4] "No Title." [Online]. Available: https://en.wikipedia.org/wiki/Cost_of_electricity_by_source.

[5] M. T. Zarmai, N. N. Ekere, C. F. Oduoza, and E. H. Amalu, "A review of interconnection technologies for improved crystalline silicon solar cell photovoltaic module assembly," *Appl. Energy*, vol. 154, pp. 173–182, 2015.

[6] A. Ndiaye, A. Charki, A. Kobi, C. M. F. Kébé, P. A. Ndiaye, and V. Sambou, "Degradations of silicon photovoltaic modules: A literature review," *Sol. Energy*, vol. 96, pp. 140–151, 2013.

[7] D. Degraaff, R. Lacerda, Z. Campeau, and S. Corp, "Degradation mechanisms in Si module technologies observed in the field; their analysis and statistics," *NREL 2011 Photovolt. Modul. Reliab. Work.*, no. February, pp. 1–25, 2011.

[8] H. Wormeester, H. J. W. Zandvliet, and B. Poelsema, "Applied Surface Science Surface adhesion and its dependence on surface roughness and humidity measured with a flat tip," vol. 258, pp. 6938–6942, 2012.

[9] R. Iea-pvps, *Assessment of Photovoltaic Module Failures in the Field*. 2017.

[10] O. O. Ogbomo, E. H. Amalu, N. N. Ekere, and P. O. Olagbegi, "A review of photovoltaic module technologies for increased performance in tropical climate," *Renew. Sustain. Energy Rev.*, vol. 75, no. September 2016, pp. 1225–1238, 2017.

[11] J. H. Wohlgemuth, P. Hacke, N. Bosco, D. C. Miller, M. D. Kempe, and S. R. Kurtz, "Assessing the causes of encapsulant delamination in PV modules," *2017 IEEE 44th Photovolt. Spec. Conf. PVSC 2017*, pp. 1–6, 2018.

[12] B. R. K. Blackman, "Handbook of Adhesion Technology," *Handb. Adhes. Technol.*, 2011.

[13] "adhesive testing instruments." [Online]. Available: https://www.caplinq.com/adhesion-primers-promoters.html?ASC.

[14] M. Müller and D. Herák, "Dimensioning of the bonded lap joint," vol. 56, no. 2, pp. 59–68,

2010.

[15] R. P. SHELDON, “Theory of Adhesion,” *Nature*, vol. 215, no. 5103, pp. 905–905, 2006.

[16] “Testing the mechanical, thermal and chemical properties of adhesives for marine environments,” 2012.

[17] W. R. Broughton, “Project PAJ3 - Combined Cyclic Loading and Hostile Environments 1996-1999 Report No 19 Project PAJ3 : Final Report,” no. 19, 1999.

[18] T. Fundamentals and A. J. Design, “adhesion ~ bonding The Fundamentals of Adhesive Joint,” no. November, pp. 55–57, 2008.

[19] K. J. Kubiak, M. C. T. Wilson, T. G. Mathia, and P. Carval, “Wettability versus roughness of engineering surfaces,” *Wear*, vol. 271, no. 3–4, pp. 523–528, 2011.

[20] “No Title.” [Online]. Available: https://cdn2.hubspot.net/hubfs/516902/Pdf/Attension/Tech Notes/AT-TN-07-Surface-roughness-CA-wettability.pdf.

[21] “No Title.”

[22] P. M. Brogly and P. Polyme, “Handbook of Adhesion Technology,” *Handb. Adhes. Technol.*, 2011.

[23] B. Lorenz *et al.*, “Adhesion: Role of bulk viscoelasticity and surface roughness,” *J. Phys. Condens. Matter*, vol. 25, no. 22, 2013.

[24] D.E. Packham, *Handbook of Adhesion*. Longman Scientific & Technical, 1993.

[25] “No Title.” [Online]. Available: http://web.mit.edu/nnf/education/wettability/rough.html.

[26] “No Title.” [Online]. Available: https://onlinelibrary.wiley.com/doi/abs/10.1002/mame.201500143.

[27] A. Venkatakrishnan and V. K. Kuppa, “ScienceDirect Polymer adsorption on rough surfaces,” *Curr. Opin. Chem. Eng.*, vol. 19, pp. 170–177, 2018.

[28] “Rheology 1,” pp. 1–22.

[29] A. Van Bael, *Industrial polymer processing [cursus]*. Diepenbeek: Gezamenlijke opleiding Industriële Ingenieurswetenschappen UHasselt & KU Leuven, 2018.

[30] “No Title.” [Online]. Available: https://wiki.anton-paar.com/en/basics-of-rheology/#oscilliation-tests-and-viscoelasticity.

[31] “No Title.” [Online]. Available: https://www.open.edu/openlearn/science-maths-technology/science/chemistry/introduction-polymers/content-section-5.3.2.

[32] T. A. Ostwald and J. Rietveld, “No Title,” in *Adhesives and sealants*, pp. 315–323.

[33] M. Herdy, “ViscoData & ViscoShift,” pp. 1–29, 2003.

[34] Y. J. Park, H. J. Kim, M. Rafailovich, and J. Sokolov, “Viscoelastic properties and lap shear strength of EVA/aromatic hydrocarbon resins as hot-melt adhesives,” *J. Adhes. Sci. Technol.*, vol. 17, no. 13, pp. 1831–1845, 2003.